NASA Technical Paper 1878

Experimental and Theoretical Supersonic Lateral-Directional Stability Characteristics of a Simplified Wing-Body Configuration With a Series of Vertical-Tail Arrangements

Milton Lamb, Wallace C. Sawyer,
and James L. Thomas

AUGUST 1981

NASA

NASA Technical Paper 1878

Experimental and Theoretical Supersonic Lateral-Directional Stability Characteristics of a Simplified Wing-Body Configuration With a Series of Vertical-Tail Arrangements

Milton Lamb, Wallace C. Sawyer,
and James L. Thomas
Langley Research Center
Hampton, Virginia

NASA
National Aeronautics
and Space Administration

**Scientific and Technical
Information Branch**

1981

SUMMARY

An experimental investigation has been conducted to provide a systematic set of lateral-directional stability data for a simplified wing-body model with a series of vertical-tail arrangements. The study was made at Mach numbers from 1.60 to 2.86 at nominal angles of attack from -8^{o} to 12^{o} and Reynolds number of 8.2×10^{6} per meter. Comparisons at zero angle of attack have been made with three existing theoretical methods (MISLIFT - a second-order shock expansion and panel method; APAS - a slender body and "first order" panel method; and PAN AIR - a "higher order" panel method) and comparisons at angle of attack have been made with PAN AIR.

The results show that PAN AIR generally provides accurate estimates of these characteristics at moderate angles of attack for complete configurations with either single or twin vertical tails. APAS provides estimates for complete configurations at zero angle of attack. However, MISLIFT only provides estimates for the simplest body—vertical-tail configurations at zero angle of attack.

INTRODUCTION

Computer codes have been developed for rapid accurate estimates of the aerodynamic characteristics of aircraft and missile configurations at supersonic speeds. Much attention has been given to the development and assessment of these methods for predicting the lift, drag, and pitching-moment characteristics of complex configurations. Many of these methods have the capability of predicting the lateral-directional characteristics of aircraft and missiles, but their utility has not been evaluated by comparison with experiment.

An effort has been initiated at NASA Langley Research Center with the primary purpose of providing experimental data on simple wing—body—vertical-tail configurations with which to assess lateral-directional stability estimating techniques at supersonic speeds. The longitudinal aerodynamic characteristics of the configurations were also recorded during the test program and are included in tabular form. These experimental data are presented along with an assessment of three of the existing methods capable of estimating lateral-directional parameters. The methods include a second-order shock expansion and panel method (MISLIFT, ref. 1), a slender body and "first order" panel method (APAS, ref. 2), and a "higher order" panel method for linearized supersonic flow (PAN AIR, ref. 3).

SYMBOLS

Force and moment data are referred to the body axis system except for lift and drag data which are referenced to the stability axis system. The moment reference center was located at 75.6 percent of the body length. The model was

designed, built, and the data were reduced using the U.S. Customary Units; however, all data are presented in the SI Units.

A	reference area, maximum cross-sectional area of body, 0.00456 m^2
AR	aspect ratio
b	wing or tail span (exposed), cm
C_D	drag coefficient, $\frac{\text{Drag}}{qA}$
C_L	lift coefficient, $\frac{\text{Lift}}{qA}$
C_l	rolling-moment coefficient, $\frac{\text{Rolling moment}}{qAd}$
C_{l_β}	effective dihedral parameter (roll stability parameter), $\left(\frac{\Delta C_l}{\Delta \beta}\right)_{\beta=0^\circ,3^\circ}$
C_m	pitching-moment coefficient, $\frac{\text{Pitching moment}}{qAl}$
C_n	yawing-moment coefficient, $\frac{\text{Yawing moment}}{qAd}$
C_{n_β}	directional stability parameter, $\left(\frac{\Delta C_n}{\Delta \beta}\right)_{\beta=0^\circ,3^\circ}$
C_Y	side-force coefficient, $\frac{\text{Side force}}{qA}$
C_{Y_β}	side-force parameter, $\left(\frac{\Delta C_Y}{\Delta \beta}\right)_{\beta=0^\circ,3^\circ}$
c_r	root chord
c_t	tip chord
d	body diameter, 7.62 cm

l	body length, 88.90 cm
M	free-stream Mach number
M.S.	model station (measured from nose), cm
q	free-stream dynamic pressure, Pa
t	panel maximum thickness, cm
α	angle of attack, deg
β	angle of sideslip, deg
Λ	leading-edge sweep angle, deg
λ	taper ratio, $\frac{c_t}{c_r}$

Model components:

B	body
V_1	vertical tail 1, body mounted
V_2	vertical tail 2, body mounted
V_3	vertical tail 3, body mounted
V_4	vertical tail 4, body mounted
V_{5-2d}	vertical tail 5, wing mounted with 2-body-diameter spacing
V_{5-4d}	vertical tail 5, wing mounted with 4-body-diameter spacing
V_{6-2d}	vertical tail 6, wing mounted with 2-body-diameter spacing
V_{6-4d}	vertical tail 6, wing mounted with 4-body-diameter spacing
W	wing

TEST PROCEDURE, MODEL, AND DATA

Test Procedure

The investigation was conducted in the low Mach number test section of the Langley Unitary Plan Wind Tunnel, which is a variable-pressure continuous-flow facility. The test section is approximately 2.13 meters long and 1.22 meters

square. For the present tests, the Mach number, stagnation pressure, and stagnation temperature were as follows:

M	Stagnation pressure, kPa	Stagnation temperature, K
1.60	68.28	339
2.36	79.43	339
2.86	123.05	339

The nominal test Reynolds number was 8.2×10^6 per meter.

The dew-point temperature measured at stagnation pressure was maintained below 239 K to assure negligible condensation effects. All tests were conducted with boundary-layer transition strips on the body 2.05 cm aft of the nose and 1.02 cm aft (measured streamwise) of the leading edges of the wing and tail surfaces. The transition strips consisted of No. 60 sand sprinkled in approximately 0.157-cm-wide strips.

Model

A two-view sketch of a typical model configuration is shown in figure 1(a). The body consisted of a 3.5 caliber tangent ogive nose followed by a cylindrical section with an overall fineness ratio of 11.67. The wings and vertical tails were removable to permit a wide variation of model configurations to be tested. Four of the configurations had a vertical tail mounted on the body, and the two other configurations had vertical tails mounted at two spanwise locations on the wings. Details of the vertical tails are given in table I and figure 1(b) and those of the wing in table I and figure 1(c). The leading and trailing edges of the tails and wings were sharp wedges having total angles measured in a plane perpendicular to the edges of 24° and 20°, respectively. The two spanwise locations for the wing mounted tails are also shown in figure 1(c).

Data Measurements and Corrections

Aerodynamic forces and moments on the model were measured by means of a six-component electrical strain-gage balance which was housed within the model. The balance was attached to a sting which was rigidly fastened to the tunnel support system. Balance chamber pressure was measured by means of a static-pressure orifice located in the vicinity of the balance.

The angles of attack were corrected for deflection of the balance and sting due to aerodynamic loads and tunnel-flow misalignment. The drag-coefficient data were adjusted to free-stream conditions acting over the model base.

THEORETICAL METHODS

MISLIFT: The MISLIFT method (ref. 1), which estimates lift-induced pressures on a wing-body combination, incorporates two separate and distinct theories. Specifically, the second-order shock-expansion theory of reference 4 is used to obtain the lifting pressures on the body alone at small angles of attack and the lifting pressures induced by a lifting surface are evaluated by the numerical solution to the linear-theory integral equations of reference 5. The numerical solution of these equations is effected by treating the planform as a planar composite of elemental rectangles and applying summation techniques to satisfy the necessary integral relations. A further description of the theoretical method and comparison with experimental results can be obtained from reference 1. This method predicts the aerodynamic characteristics for a planar-type configuration. And, for the present study, the model was taken to be a planar configuration in the side view in order to estimate the lateral-directional characteristics.

APAS: The Aerodynamic Preliminary Analysis System (ref. 2) is a "first order" panel method solution for linearized subsonic and supersonic flight. Angle of attack and sideslip solutions are handled independently. A general slender-body theory is used to represent body-alone effects. The perturbation velocities from the body are included in a Woodward "constant pressure" analysis method for thin lifting surfaces. Interference shells are used in the lifting-surface analysis to carry over the load from the wings onto the body. The lifting-surface method uses a vortex singularity of constant strength in the chordwise direction on each of the panels into which the lifting surfaces are divided. The loads on the lifting surfaces are calculated directly from the solution using the first-order pressure-coefficient relation, accounting for only the perturbation velocities in the free-stream direction. The total forces and moments are a sum of the slender-body and lifting-surface solutions.

PAN AIR: The PAN AIR pilot code (ref. 3) is a "higher order" panel method solution for linearized subsonic and supersonic flow. Combined source and doublet panels with linearly varying source and quadratically varying doublet distributions can be used. The quadrilateral panels formed from a rectangular array of input points are each divided into eight triangular flat subpanels in such a way that all panel edges are contiguous with adjacent panels. Quadratic doublet distributions over each triangular subpanel are prescribed, leading to a continuous piecewise quadratic doublet strength over the entire configuration. The source strength is not required to be continuous and a linear least-square type of distribution is used.

This method allows a wide variety of singularity and boundary-condition formulations to be specified including both chord plane and surface panel modeling options. For "thick" body type of solutions a common approach is to use combined source and doublet panels with a perturbation potential boundary condition corresponding to zero normal mass flux through the surface. For "thin" wings, thickness effects can be considered to be secondary and doublets alone can be used on the lifting surfaces to satisfy zero normal mass flux through the surface. A combination of these two approaches was used in the present application: combined source and doublet panels were used on the body and doublet panels were used on the wings and vertical tails. In the context of small-

perturbation solution, a distinction between zero normal mass flux and zero normal velocity flux can be made. Based on previous experience (ref. 6), the formulation corresponding to zero normal velocity flux was used on the body and that corresponding to zero normal mass flux was used on the wing and tail surfaces. Also within the context of the small-perturbation solution, compressibility axes can be defined which are not aligned with free-stream direction. In all of the results presented, however, compressibility axes were aligned with the free-stream direction.

The forces and moments are calculated by integrating the pressure coefficient over the surface. The isentropic pressure relation was used to calculate the pressure coefficient from the total velocity.

DISCUSSION

The experimental longitudinal characteristics are presented in table II. The experimental lateral-directional stability data are presented in figures 2 to 5. The comparisons of experimental and theoretical lateral-directional stability parameters at $\alpha = 0^{\circ}$ are presented in figure 6 for the various configurations. As was previously noted, MISLIFT is a planar solution and, therefore, only configurations which have lifting surfaces in a single plane could be analyzed by this method; however, both the APAS and PAN AIR codes could be used to analyze complete configurations. The B, BW, and BWV_1 configurations are shown in figures 6(a) to 6(c). The theoretical estimates of C_{Y_β} and C_{l_β} show fair to good agreement with the experimental results, except for C_{l_β} of the BWV_1 configuration (fig. 6(c)) at $M = 2.86$, which probably results from the scatter of experimental data as shown in figure 2(c). Fair agreement is shown for C_{n_β} for either MISLIFT or PAN AIR. Both MISLIFT and PAN AIR show a variation of all parameters with Mach number, whereas APAS, which is based on a slender-body theory for the body effects, does not show this variation with Mach number for the B or BW configuration but does show a variation with Mach number for the BWV_1 configuration. The APAS results for the BW configuration are the same as the results for the B configuration, and indeed the experimental data show little effect of addition of the wing at $\alpha = 0^{\circ}$. The body—vertical-tail configurations are shown in figures 6(d) to 6(g). Fair to good comparisons are made for C_{Y_β} and C_{l_β} for all configurations with only slight differences among the three theories. Fair to good agreement in C_{n_β} is shown for MISLIFT and PAN AIR, except for BV_3 (fig. 6(f)). This exception is probably due to the increase in moment arm which tends to magnify any error in the side force or center-of-pressure location. Comparisons for the wing-mounted vertical-tail configurations are shown in figures 6(h) to 6(k). Fair to good agreement is shown for all parameters for PAN AIR.

Since the results from MISLIFT and APAS are invariant with angle of attack, only the results from PAN AIR are used for comparisons of the stability parameters at angles of attack. These comparisons are shown in figure 7 for the vari-

ous configurations. It should be noted that the theory is violated at $M = 2.86$ for $\alpha \gtrsim 5^{\circ}$. Overall, the results are quite good, except for the BWV_{6-2d} and BWV_{6-4d} configurations (figs. 7(f) and 7(g)). The difference may be attributed to the inability of the program to account for the presence of vortices, etc.

CONCLUDING REMARKS

An effort has been initiated at NASA Langley Research Center to assess three existing methods of estimating lateral-directional stability characteristics at supersonic speeds. The prediction methods include a second-order shock expansion and panel method (MISLIFT), a slender-body and "first order" panel method (APAS), and a "higher order" panel method for linearized supersonic flow (PAN AIR). The results lead to the following concluding remarks:

1. PAN AIR generally provides accurate predictions at moderate angles of attack for complete configurations with either single or twin vertical tails.

2. APAS will provide fairly accurate predictions at zero angle of attack for complete configurations with either single or twin vertical tails.

3. MISLIFT will only provide estimates for the simplest body—vertical-tail configurations at zero angle of attack.

Langley Research Center
National Aeronautics and Space Administration
Hampton, VA 23665
June 9, 1981

REFERENCES

1. Jackson, Charlie M., Jr.; and Sawyer, Wallace C.: A Method for Calculating the Aerodynamic Loading on Wing-Body Combinations at Small Angles of Attack in Supersonic Flow. NASA TN D-6441, 1971.

2. Bonner, E.; Clever, W.; and Dunn, K.: Aerodynamic Preliminary Analysis System. Part I - Theory. Contract NAS1-14686, Los Angeles Div., Rockwell International Corp., 1978. (Available as NASA CR-145284.)

3. Ehlers, F. E.; Epton, M. A.; Johnson, F. T.; Magnus, A. E.; and Rubbert, P. E.: An Improved Higher Order Panel Method for Linearized Supersonic Flow. AIAA Paper No. 78-15, Jan. 1978.

4. Syvertson, Clarence A.; and Dennis, David H.: A Second-Order Shock-Expansion Method Applicable to Bodies of Revolution Near Zero Lift. NACA Rep. 1328, 1957. (Supersedes NACA TN 3527.)

5. Middleton, Wilbur D.; and Carlson, Harry W.: A Numerical Method for Calculating the Flat-Plate Pressure Distributions on Supersonic Wings of Arbitrary Planform. NASA TN D-2570, 1965.

6. Thomas, James L.; and Miller, David S.: Numerical Comparisons of Panel Methods at Subsonic and Supersonic Speeds. AIAA Paper 79-0404, Jan. 1979.

TABLE I.- COMPONENT CHARACTERISTICS

Component designation	Λ, deg	Area, cm^2	λ	AR	b, cm	t, cm
Vertical tails						
V_1	60	203.2	0.50	0.88	13.34	0.79
V_2	60	203.2	.14	.88	13.34	.79
V_3	65	203.2	.50	.88	13.34	.79
V_4	60	203.2	.50	.49	10.00	.79
V_5	60	[a]101.6	.50	[a].88	[a]9.43	.48
V_6	60	[a]203.2	.50	[a].88	[a]13.34	.48
Wing						
W	68	[b]1153.7	0.00	[b]1.62	[b]43.18	0.95

[a]Based on exposed single panel.
[b]Based on exposed double panel.

TABLE II.- LONGITUDINAL STABILITY CHARACTERISTICS

M = 1.60				M = 2.00				M = 2.86			
α, deg	C_L	C_D	C_m	α, deg	C_L	C_D	C_m	α, deg	C_L	C_D	C_m
B configuration											
-6.31	-0.2979	0.2421	-0.1545	-6.30	-0.3029	0.2254	-0.1458	-6.34	-0.4267	0.2129	-0.2085
-4.26	-.1704	.2187	-.0983	-4.25	-.1713	.2013	-.0824	-4.28	-.2428	.1783	-.1364
-2.22	-.0838	.2032	-.0413	-2.19	-.0838	.1912	-.0281	-2.22	-.1103	.1638	-.0746
-1.19	-.0407	.2016	-.0153	-1.18	-.0394	.1857	-.0001	-1.20	-.0567	.1637	-.0448
-.16	.0016	.1990	.0076	-.15	-.0163	.1866	.0279	-.18	-.0040	.1614	-.0205
.87	.0453	.2011	.0367	.88	.0495	.1889	.0576	.84	.0504	.1583	.0131
1.89	.0880	.2038	.0612	1.90	.0945	.1922	.0887	1.86	.0781	.1604	.0411
3.95	.1944	.2179	.1147	3.97	.2047	.2061	.1494	3.93	.2125	.1743	.1120
6.01	.3224	.2391	.1754	6.03	.3783	.2369	.2159	5.99	.3942	.2105	.1749
8.08	.4919	.2767	.2397	8.12	.5950	.2824	.2980	8.06	.6028	.2557	.2527
10.15	.7013	.3319	.3117	10.23	.8957	.3533	.3987	10.14	.9578	.3463	.3398
BW configuration											
-6.97	-8.9599	1.5534	0.0150	-6.16	-6.6328	1.1167	-0.0230	-7.06	-5.5086	1.0301	-0.1209
-4.56	-5.7796	.9399	.0179	-3.80	-3.9982	.6948	.0010	-4.89	-3.9582	.6910	-.0925
-2.16	-2.6236	.6184	.0141	-1.46	-1.4114	.4978	.0056	-2.67	-2.2063	.4606	-.0627
-.97	-1.1692	.5646	.0111	-.33	-.3166	.4723	.0084	-1.57	-1.2693	.4068	-.0467
.21	.1833	.5480	.0095	.83	.8229	.4818	.0127	-.46	-.3324	.3825	-.0327
1.40	1.6377	.5795	.0050	1.98	2.1072	.5257	.0157	.66	.5530	.3849	-.0112
2.58	3.1745	.6613	.0006	3.16	3.4144	.6275	.0218	1.74	1.4608	.4102	-.0027
5.00	6.3463	1.0329	-.0023	5.49	5.9703	.9882	.0399	3.98	3.1575	.5737	.0250
7.38	9.4644	1.6858	.0005	7.81	8.3944	1.5696	.0652	6.13	4.9872	.8803	.0487
9.03	12.5975	2.6368	.0156	10.18	10.7949	2.3610	.0998	8.38	6.6909	1.3374	.0983
12.24	15.4668	3.7986	.0458	12.51	13.0564	3.3188	.1499	10.58	8.3879	1.9284	.1368

TABLE II.- Continued

M = 1.60				M = 2.00				M = 2.86			
α, deg	C_L	C_D	C_m	α, deg	C_L	C_D	C_m	α, deg	C_L	C_D	C_m
BWV$_1$ configuration											
-6.95	-9.1707	1.6683	0.0595	-6.17	-6.8443	1.2263	0.0092	-6.94	-5.5592	1.1139	-0.0554
-4.55	-5.9981	1.0484	.0599	-3.80	-4.2607	.7932	.0215	-4.77	-3.9841	.7693	-.0274
-2.13	-2.7939	.7162	.0497	-1.48	-1.7206	.5837	.0289	-2.59	-2.2187	.5496	-.0013
-.97	-1.3640	.6521	.0436	-.33	-.5423	.5502	.0349	-1.44	-1.2647	.4854	.0129
.23	.0868	.6379	.0391	.81	.6339	.5515	.0300	-.38	-.4790	.4613	.0248
1.40	1.4523	.6628	.0344	1.97	1.8749	.5942	.0345	.74	.3251	.4586	.0349
2.59	2.9409	.7330	.0285	3.15	3.1818	.6803	.0390	1.83	1.4347	.4538	.0511
5.00	6.1381	1.0971	.0270	5.49	5.7778	1.0366	.0570	4.05	3.2032	.6451	.0753
7.43	9.3396	1.7531	.0281	7.82	8.2596	1.6119	.0790	6.22	4.8252	.9329	.1021
9.82	12.3193	2.6612	.0398	10.17	10.6330	2.3854	.1120	8.49	6.6233	1.3922	.1347
12.24	15.2540	3.8269	.0638	12.49	12.8776	3.3291	.1666	10.67	8.2419	1.9653	.1656
BV$_1$ configuration											
-9.29	-0.4096	0.3746	-0.1858	-7.19	-0.3674	0.3324	-0.1937	-8.51	-0.5000	0.3286	-0.2134
-7.24	-.2887	.3338	-.1291	-5.11	-.2409	.3001	-.1329	-6.45	-.3244	.2710	-.1482
-5.19	-.2079	.3074	-.0785	-3.07	-.1574	.2811	-.0801	-4.41	-.1963	.2474	-.0885
-4.17	-.1665	.2999	-.0525	-2.08	-.1147	.2775	-.0537	-3.37	-.1433	.2396	-.0550
-3.15	-.1254	.2911	-.0280	-1.03	-.0729	.2700	-.0289	-2.35	-.0914	.2350	-.0252
-2.12	-.0845	.2865	-.0004	.00	-.0297	.2673	-.0009	-1.33	-.0400	.2283	-.0009
-1.09	-.0427	.2832	.0240	1.04	.0129	.2670	.0255	-.31	-.0136	.2241	.0270
.97	.0618	.2816	.0775	3.10	.1414	.2810	.0860	1.75	.1174	.2313	.0942
3.02	.1877	.2949	.1357	5.15	.2920	.3006	.1528	3.79	.2730	.2484	.1520
5.10	.3543	.3141	.1988	7.26	.5048	.3375	.2351	5.87	.5038	.2883	.2265
7.17	.5323	.3482	.2746	9.35	.7925	.4001	.3366	7.96	.8231	.3504	.3187

TABLE II.- Continued

M = 1.60				M = 2.00				M = 2.86			
α, deg	C_L	C_D	C_m	α, deg	C_L	C_D	C_m	α, deg	C_L	C_D	C_m
BV_2 configuration											
-6.27	-0.2851	0.3521	-0.1499	-6.81	-0.3284	0.3288	-0.1960	-7.53	-0.4599	0.3044	-0.2355
-4.21	-.1610	.3277	-.0877	-4.73	-.2022	.2994	-.1316	-5.45	-.3052	.2639	-.1670
-2.16	-.0789	.3126	-.0323	-2.66	-.0967	.2850	-.0756	-3.38	-.1771	.2350	-.1017
-1.15	.0388	.3079	-.0092	-1.63	-.0757	.2801	-.0492	-2.37	-.1243	.2287	-.0699
-.14	.0030	.3025	.0153	-.61	-.0329	.2746	-.0182	-1.35	-.0724	.2254	-.0438
.92	.0654	.3018	.0430	.42	.0097	.2747	.0097	-.32	-.0203	.2223	-.0140
1.92	.1062	.3055	.0676	1.45	.0738	.2776	.0392	.69	.0057	.2245	-.0103
3.96	.1884	.3166	.1228	3.49	.1797	.2903	.0966	2.76	.1359	.2327	.0736
6.00	.3121	.3394	.1776	5.54	.3497	.3143	.1614	4.80	.2659	.2547	.1364
8.10	.4769	.3785	.2431	7.56	.5634	.3570	.2463	6.88	.4984	.2928	.2160
10.18	.6636	.4276	.3224	9.79	.8625	.4284	.3529	8.97	.8555	.3689	.3050
BV_3 configuration											
-7.65	-0.3798	0.3440	-0.1822	-7.17	-0.3662	0.3311	-0.1988	-8.48	-0.5259	0.3234	-0.2089
-5.61	-.2576	.3107	-.1322	-5.13	-.2431	.2943	-.1424	-6.43	-.3515	.2668	-.1520
-3.58	-.1545	.2889	-.0762	-3.07	-.1377	.2725	-.0872	-4.36	-.2462	.2418	-.0821
-2.56	-.1130	.2839	-.0536	-2.03	-.0952	.2695	-.0611	-3.37	-.1962	.2302	-.0639
-1.55	-.0718	.2787	-.0279	-1.01	-.0522	.2657	-.0334	-2.34	-.1188	.2200	-.0345
-.50	-.0300	.2749	-.0013	.01	-.0094	.2628	-.0066	-1.32	-.0930	.2141	-.0099
.54	.0115	.2729	.0248	1.05	.0339	.2622	.0235	-.28	-.0395	.2114	.0222
2.57	.1165	.2825	.0793	3.12	.1632	.2741	.0865	1.75	.0907	.2144	.0809
4.62	.2427	.2987	.1358	5.17	.3131	.2969	.1498	3.80	.2222	.2282	.1491
6.72	.4093	.3321	.2014	7.26	.5069	.3309	.2304	5.89	.4540	.2630	.2230
8.81	.5973	.3749	.2788	9.36	.7856	.3966	.3310	7.97	.7893	.3308	.3210

TABLE II.- Continued

M = 1.60				M = 2.00				M = 2.86			
α, deg	C_L	C_D	C_m	α, deg	C_L	C_D	C_m	α, deg	C_L	C_D	C_m
BV_4 configuration											
-6.31	-0.3077	0.3286	-0.1476	-6.80	-0.3118	0.3054	-0.1977	-6.29	-0.3888	0.2758	-0.1838
-4.25	-.1848	.3008	-.0933	-4.74	-.1845	.2767	-.1347	-4.25	-.2357	.2404	-.1214
-2.20	-.1027	.2875	-.0421	-2.67	-.0993	.2647	-.0780	-2.19	-.1316	.2237	-.0606
-1.17	-.0608	.2809	-.0119	-1.65	-.0564	.2628	-.0504	-1.17	-.0539	.2197	-.0331
-.13	-.0191	.2807	.0138	-.63	-.0138	.2592	-.0259	-.15	-.0287	.2165	-.0112
.88	.0225	.2803	.0398	.40	.0086	.2573	-.0067	.87	.0263	.2156	-.0298
1.91	.0646	.2819	.0674	1.43	.0732	.2596	.0347	1.90	.0790	.2161	.0596
3.97	.1688	.2888	.1211	3.49	.1806	.2703	.0954	3.94	.2082	.2284	.1101
6.02	.2938	.3121	.1793	5.55	.3518	.2971	.1623	5.99	.3393	.2508	.1793
8.09	.4590	.3481	.2406	7.65	.5458	.3361	.2463	8.08	.5689	.3027	.2554
10.17	.6455	.3975	.3231	9.76	.8436	.4081	.3503	10.17	.9508	.3932	.3544
BWV_{5-2d} configuration											
-6.98	-9.1712	1.7011	0.0616	-6.10	-6.7854	1.2248	0.0129	-6.98	-5.7245	1.1402	-0.0497
-4.58	-6.0535	1.0754	.0635	-3.75	-4.2400	.8022	.0281	-4.77	-3.9083	.7616	-.0179
-2.17	-2.8960	.7390	.0534	-1.43	-1.6995	.5941	.0325	-2.55	-2.0976	.5377	.0065
-.98	-1.4036	.6734	.0489	-.26	-.4580	.5569	.0354	-1.46	-1.2883	.4858	.0223
.19	-.0586	.6479	.0412	.89	.7207	.5612	.0383	-.36	-.4295	.4568	.0307
1.38	1.4335	.6683	.0388	2.04	1.9621	.6020	.0386	.75	.5327	.4613	.0472
2.57	2.9442	.7411	.0302	3.21	3.2663	.6962	.0467	1.84	1.4149	.4878	.0580
4.98	6.1034	1.1057	.0248	5.56	5.8612	1.0593	.0639	4.05	3.2334	.6493	.0850
7.37	9.2094	1.7425	.0276	7.88	8.2795	1.6351	.0861	6.26	5.0091	.9518	.1159
9.80	12.2857	2.6656	.0396	10.23	10.6797	2.4131	.1269	8.48	6.7130	1.4048	.1525
12.21	15.1490	3.8051	.0742	12.57	12.8817	3.3527	.1924	10.67	8.3559	1.9751	.1872

TABLE II.- Continued

M = 1.60				M = 2.00				M = 2.86			
α, deg	C_L	C_D	C_m	α, deg	C_L	C_D	C_m	α, deg	C_L	C_D	C_m
BWV_{5-4d} configuration											
-6.96	-9.0788	1.6721	0.0663	-6.09	-6.7396	1.2160	0.0061	-6.98	-5.6773	1.1340	-0.0495
-4.58	-5.9755	1.0662	.0606	-3.74	-4.1768	.7934	.0246	-4.78	-4.0337	.7751	-.0217
-2.17	-2.8057	.7383	.0566	-1.42	-1.6162	.5887	.0290	-2.56	-2.1240	.5384	.0047
-.98	-1.3804	.6735	.0537	-.27	-.4170	.5540	.0303	-1.45	-1.2394	.4794	.0168
.20	.0657	.6504	.0477	.88	.7407	.5620	.0316	-.35	-.2783	.4552	.0384
1.38	1.4705	.6713	.0420	2.04	2.0253	.6042	.0366	.74	.4047	.4548	.0451
2.57	2.9992	.7476	.0380	3.22	3.3515	.7016	.0400	1.86	1.4419	.4770	.0562
4.98	6.1435	1.1008	.0282	5.56	5.9452	1.0565	.0495	4.05	3.2527	.6296	.0794
7.40	9.3570	1.7335	.0310	7.89	8.4304	1.6263	.0749	6.25	4.9299	.9270	.1010
9.81	12.3209	2.6151	.0413	10.23	10.7706	2.3954	.1141	8.47	6.7103	1.3831	.1395
12.20	15.2071	3.7401	.0700	12.57	13.0500	3.3556	.1610	10.66	8.4494	1.9815	.1741
BWV_{6-2d} configuration											
-7.06	-9.3514	1.8105	0.0737	-6.16	-6.9670	1.3392	0.0128	-7.03	-5.8652	1.2239	-0.0367
-4.64	-6.1770	1.1685	.0788	-3.84	-4.4471	.9034	.0295	-4.80	-3.9711	.8316	-.0048
-2.22	-2.9954	.8176	.0701	-1.49	-1.8026	.6766	.0386	-2.63	-2.1700	.6011	.0158
-1.04	-1.5049	.7453	.0595	-.34	-.6048	.6321	.0368	-1.53	-1.4127	.5382	.0278
.13	-.1378	.7198	.0566	.81	.5716	.6350	.0397	-.40	-.4780	.5099	.0399
1.32	1.3157	.7355	.0491	1.98	1.8556	.6711	.0458	.68	.4810	.5044	.0596
2.52	2.8098	.8058	.0430	3.15	3.2025	.7633	.0504	1.81	1.4897	.5312	.0627
4.95	6.0786	1.1692	.0356	5.50	5.7937	1.1168	.0639	4.03	3.2505	.6842	.0886
7.32	9.1431	1.7938	.0369	7.84	8.3064	1.7025	.0924	6.20	4.9181	.9780	.1177
9.75	12.2000	2.7062	.0504	10.19	10.6136	2.4675	.1270	8.42	6.7124	1.4365	.1507
12.16	15.0731	3.8397	.0821	12.51	12.8005	3.3803	.1786	10.62	8.1094	1.9565	.1777

Table II.- Concluded

M = 1.60				M = 2.00				M = 2.86			
α, deg	C_L	C_D	C_m	α, deg	C_L	C_D	C_m	α, deg	C_L	C_D	C_m
BWV_{6-4d} configuration											
-7.06	-9.3914	1.7707	0.0996	-6.21	-7.1721	1.3232	0.0208	-7.03	-5.8504	1.2084	-0.0392
-4.59	-6.1578	1.1322	.0886	-3.85	-4.5543	.8730	.0368	-4.82	-4.1308	.8317	-.0067
-2.19	-2.9784	.7935	.0696	-1.48	-1.9127	.6467	.0356	-2.61	-2.2470	.5820	.0128
-1.06	-1.5073	.7276	.0656	-.35	-.7344	.6064	.0374	-1.53	-1.3929	.5250	.0236
.13	-.0976	.7010	.0613	.81	.4842	.6040	.0376	-.41	-.4045	.4889	.0420
1.31	1.2864	.7175	.0521	1.97	1.7049	.6384	.0389	.67	.3036	.4830	.0577
2.49	2.8388	.7847	.0493	3.12	3.0279	.7214	.0435	1.78	1.2650	.5030	.0680
4.88	5.9580	1.1054	.0388	5.47	5.6883	1.0545	.0539	4.00	3.1773	.6500	.0869
7.31	9.2476	1.7313	.0387	7.81	8.1952	1.6109	.0746	6.20	4.8085	.9280	.1140
9.73	12.2199	2.6083	.0460	10.17	10.6193	2.3805	.1108	8.43	6.7116	1.3908	.1415
12.14	15.1542	3.7493	.0763	12.51	12.9247	3.3310	.1624	10.62	8.3366	1.9632	.1762

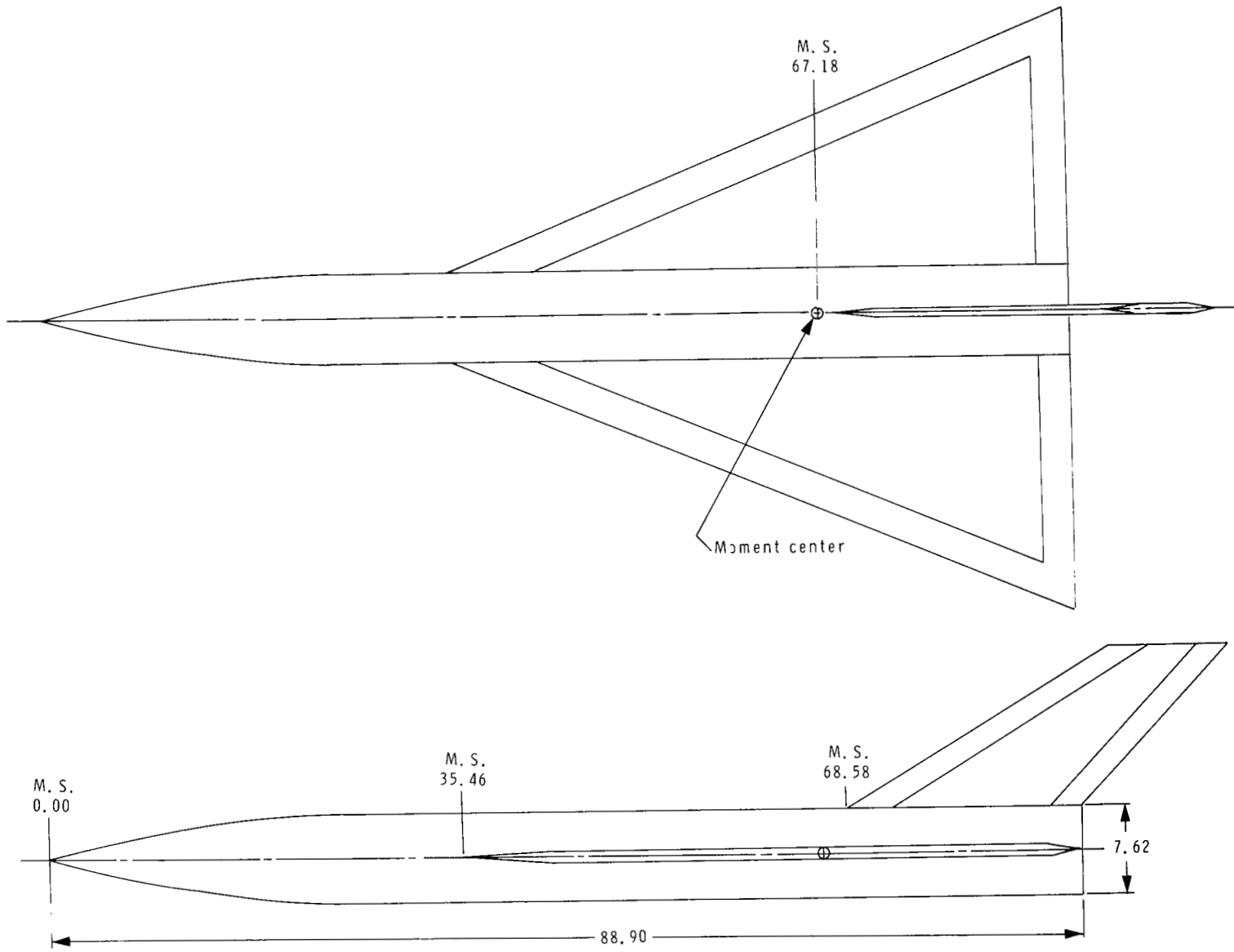

(a) Two view sketch of model BWV_1.

Figure 1.- Details of model. All linear dimensions are in centimeters.

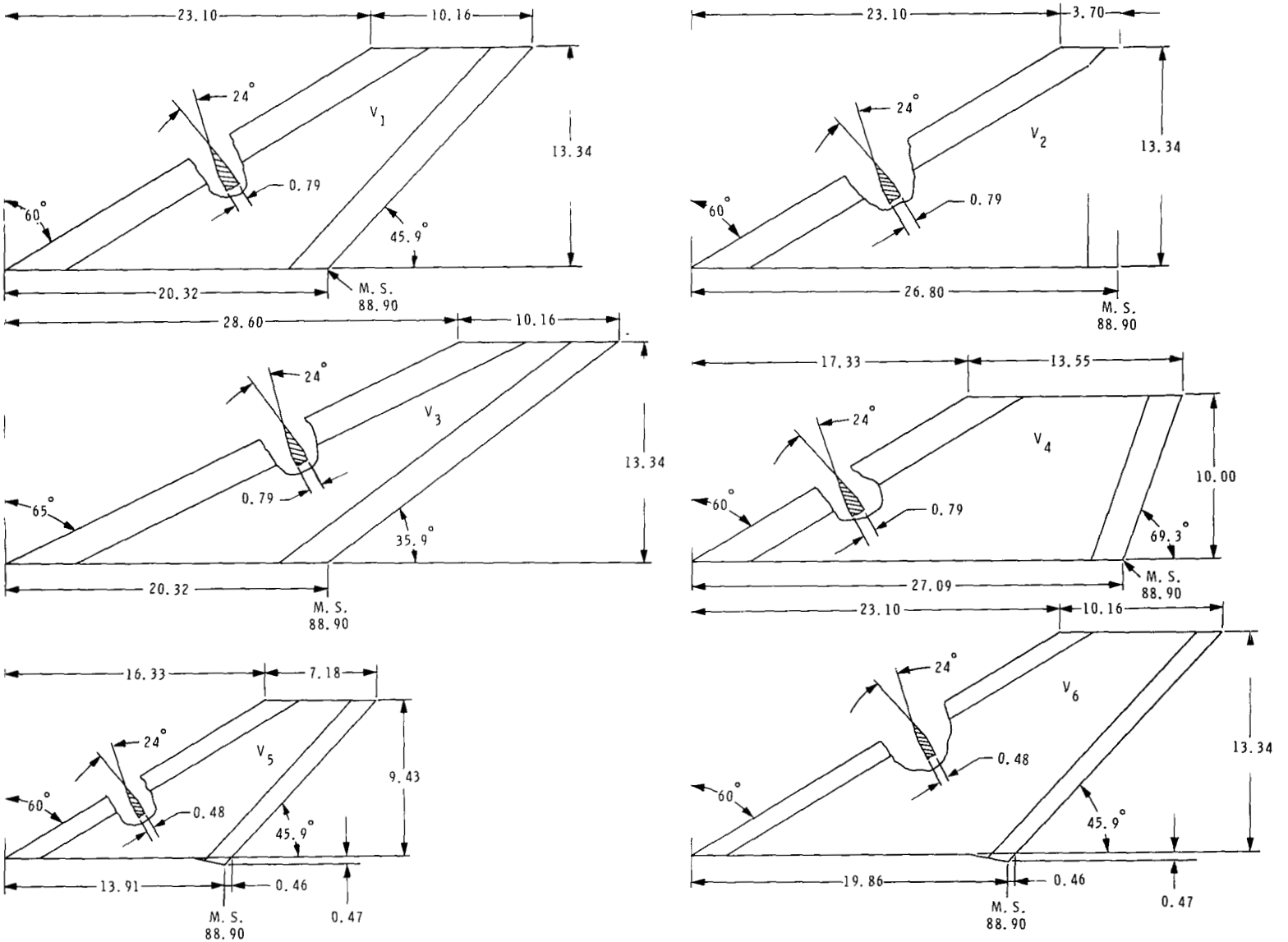

(b) Details of vertical tails.

Figure 1.- Continued.

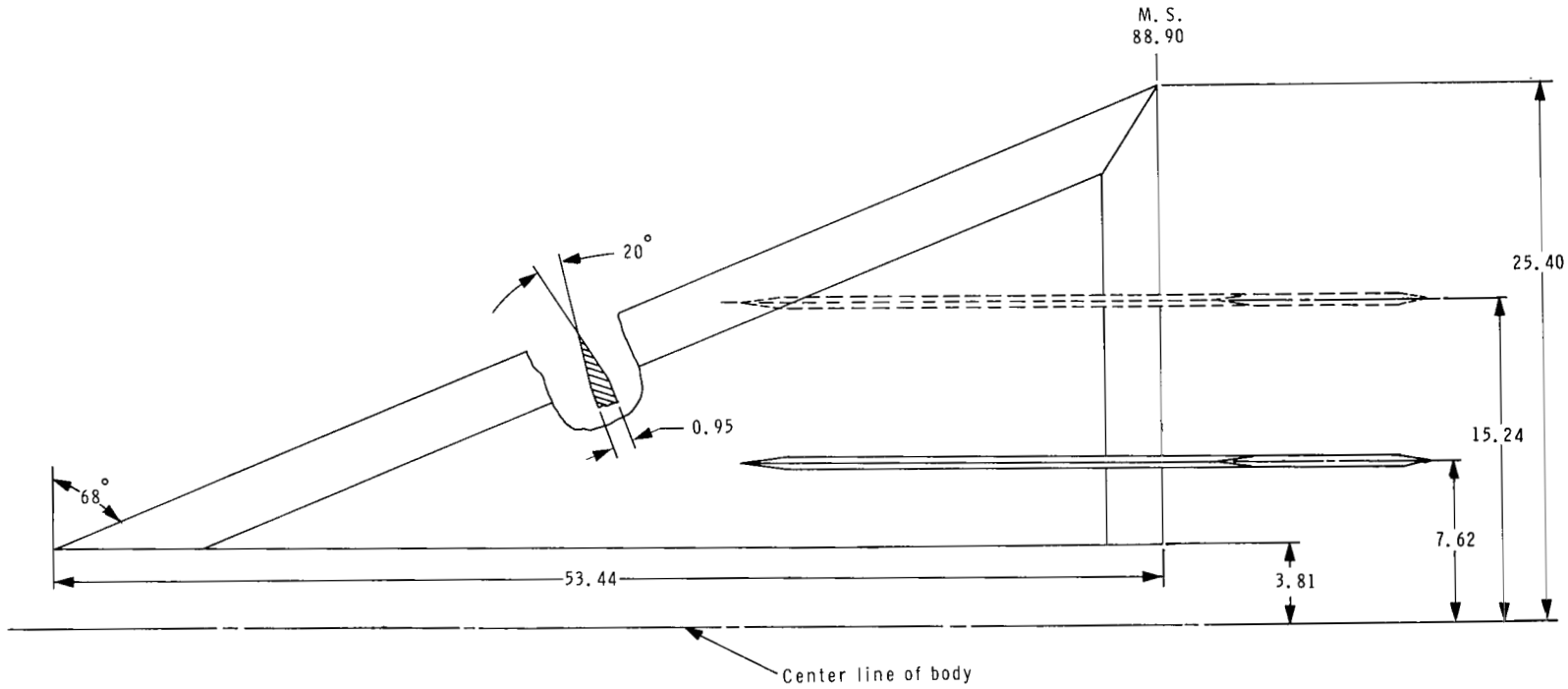

(c) Details of wing with spanwise locations of V_5 and V_6 indicated. V_5 and V_6 can be installed at either location.

Figure 1.- Concluded.

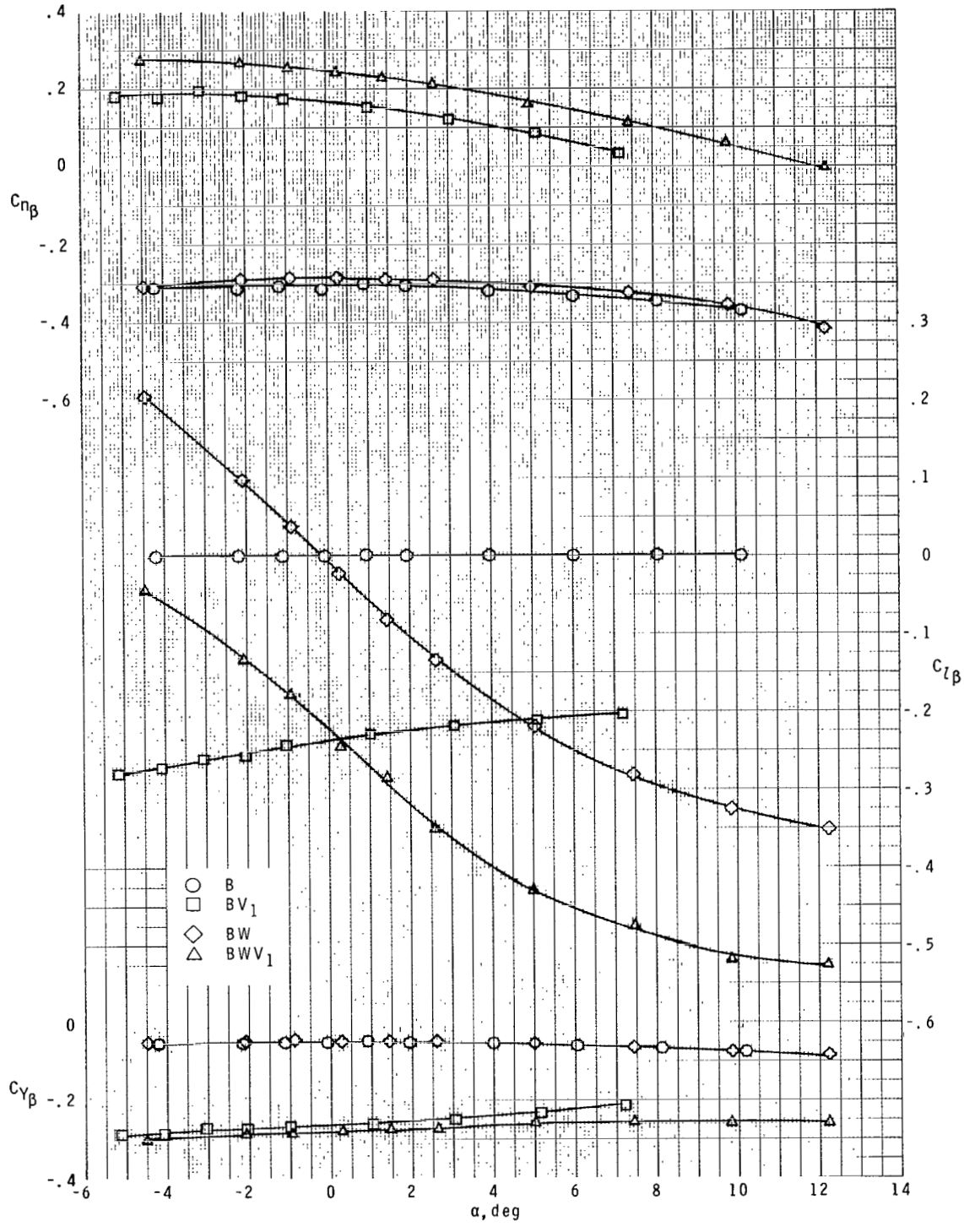

(a) M = 1.60.

Figure 2.- Effect of various components on lateral-directional stability characteristics.

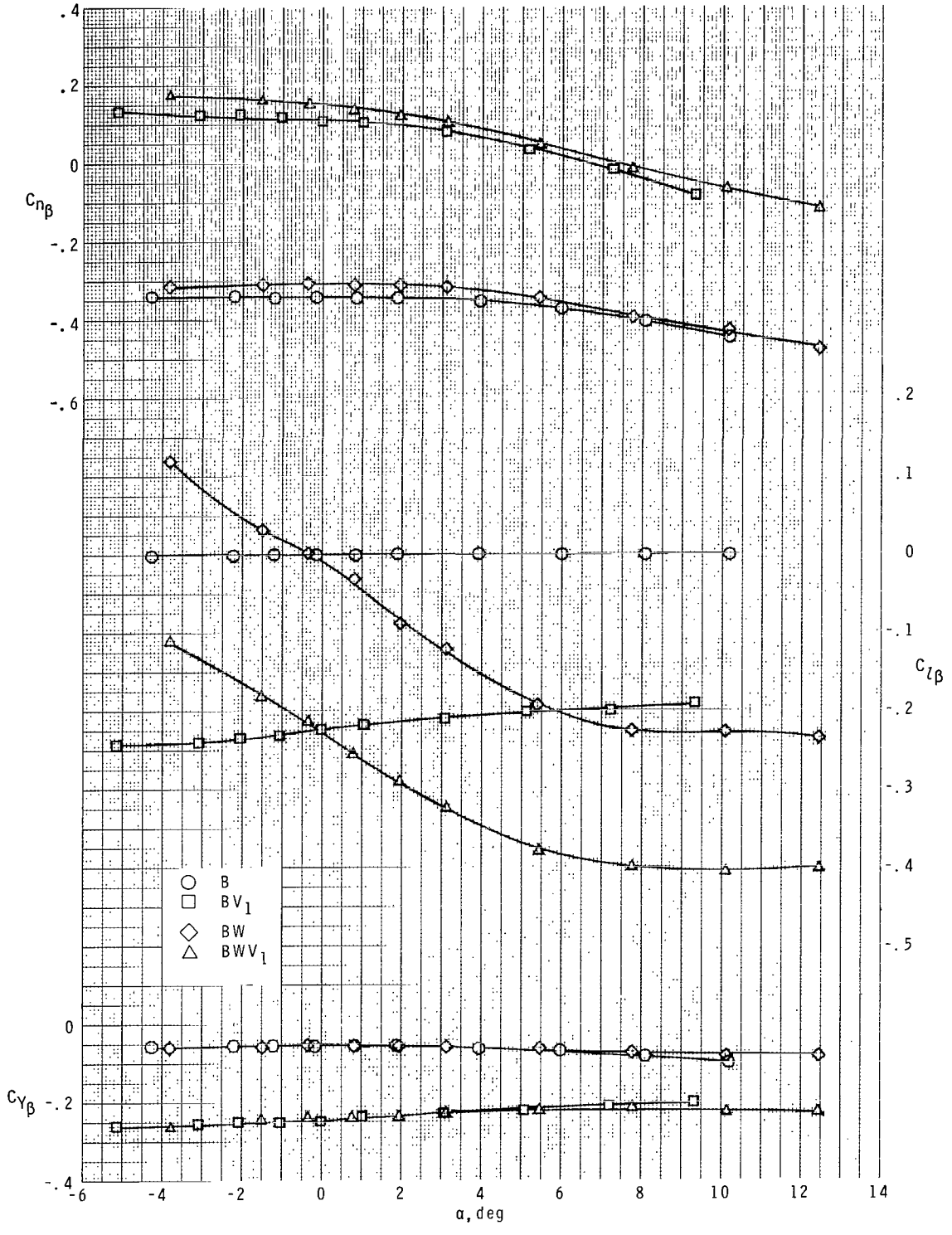

(b) M = 2.00.

Figure 2.- Continued.

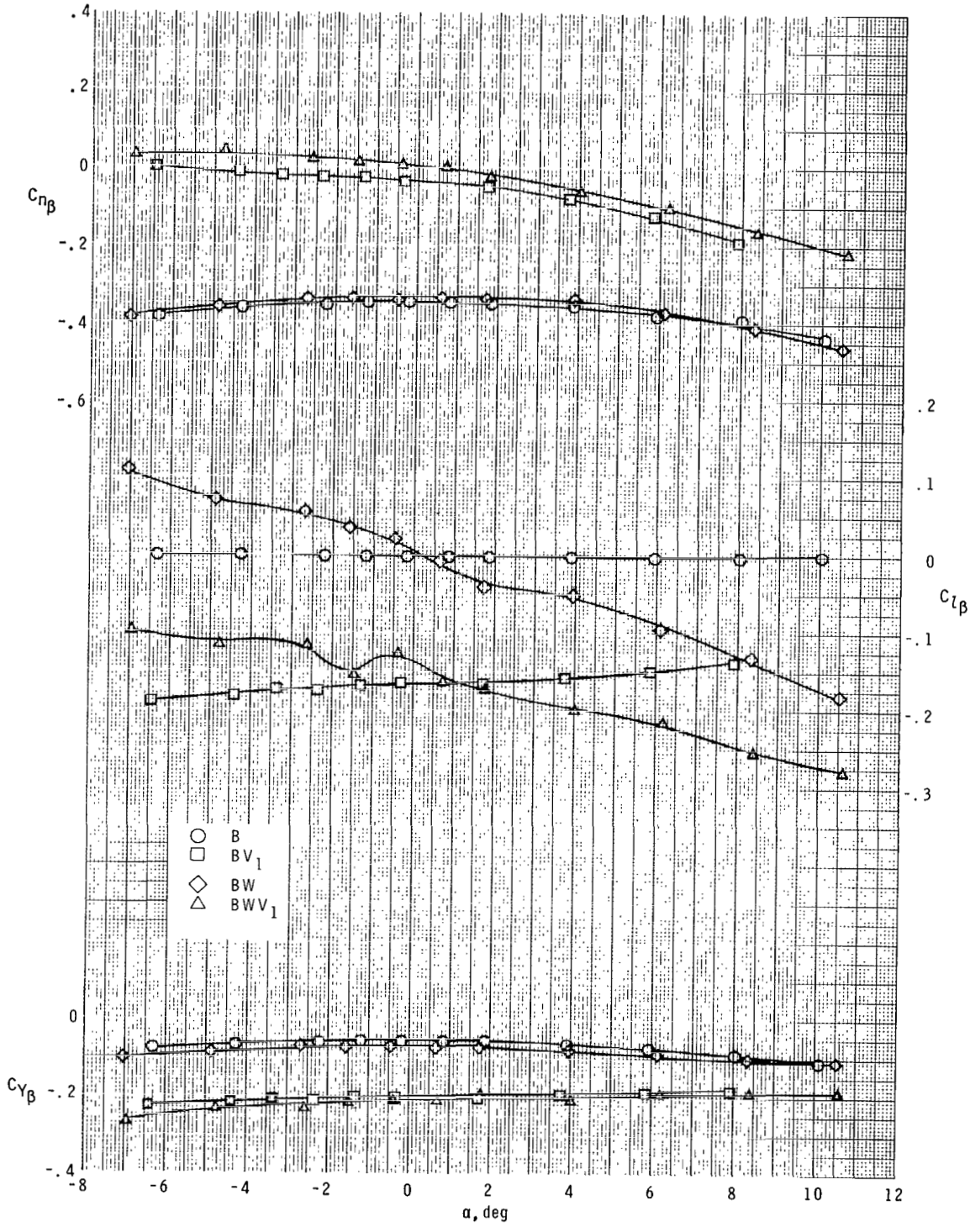

(c) M = 2.86.

Figure 2.- Concluded.

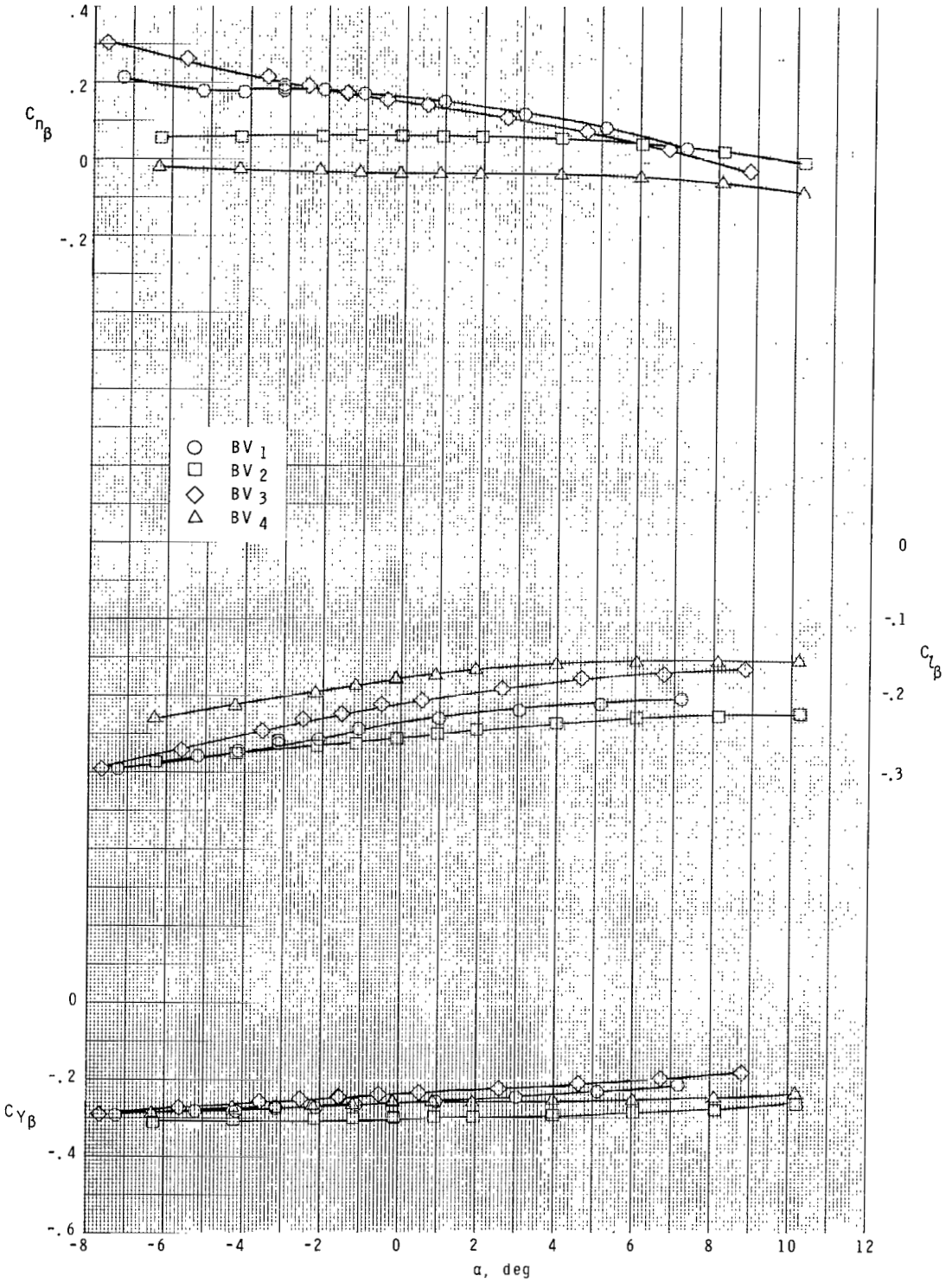

(a) M = 1.60.

Figure 3.- Effect of various vertical tails on lateral-directional stability characteristics.

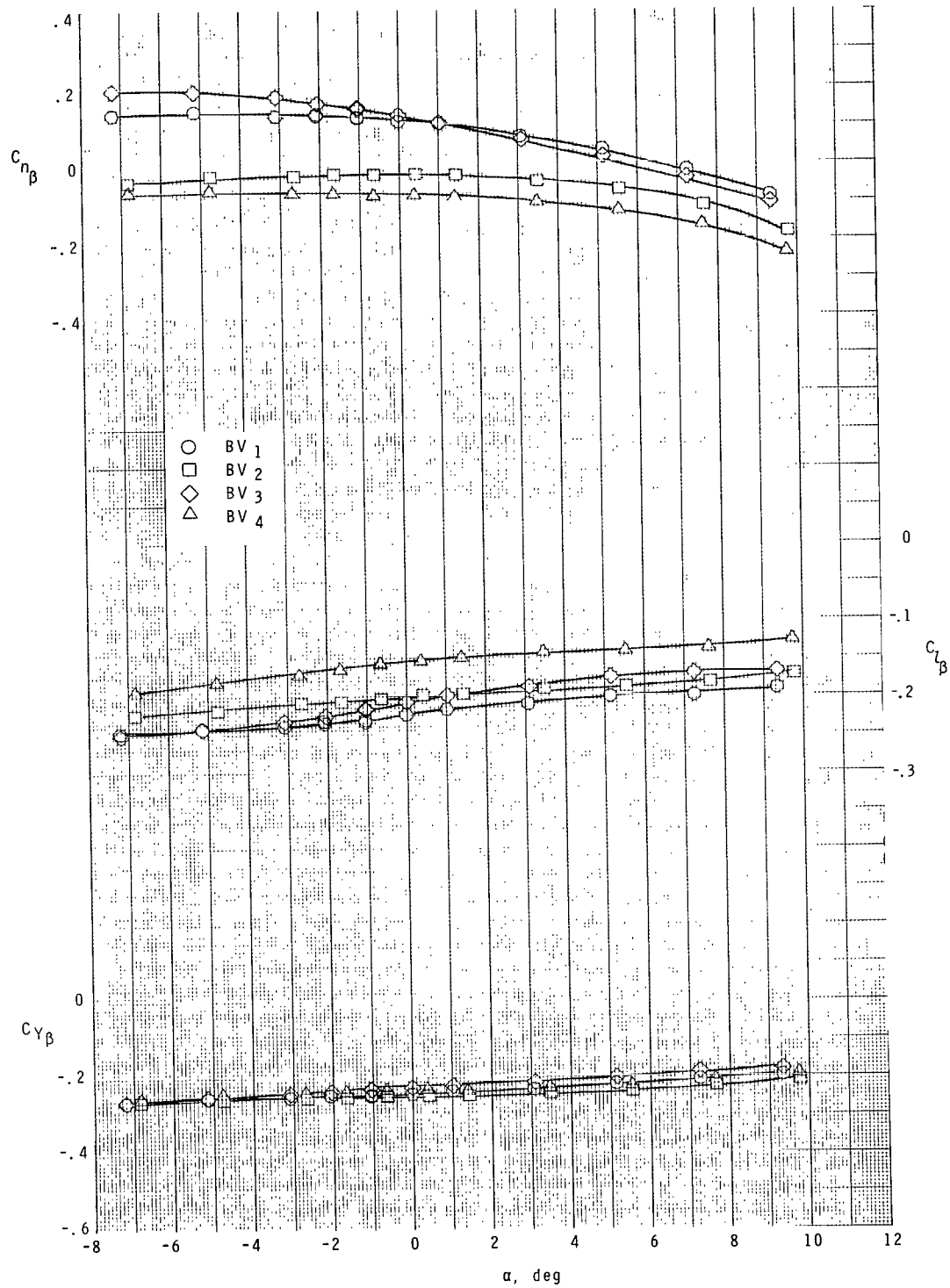

(b) M = 2.00.

Figure 3.- Continued.

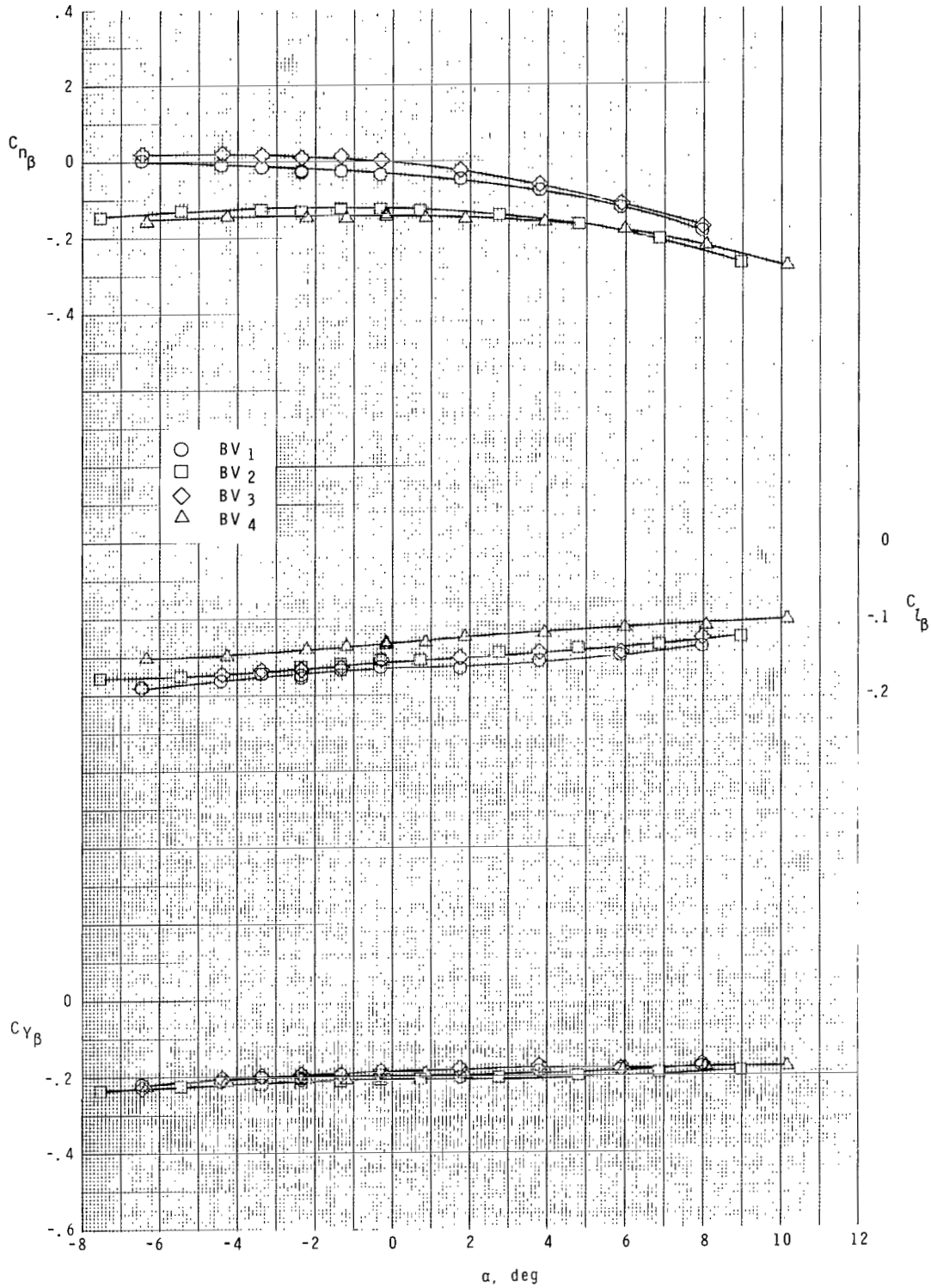

(c) M = 2.86.

Figure 3.- Concluded.

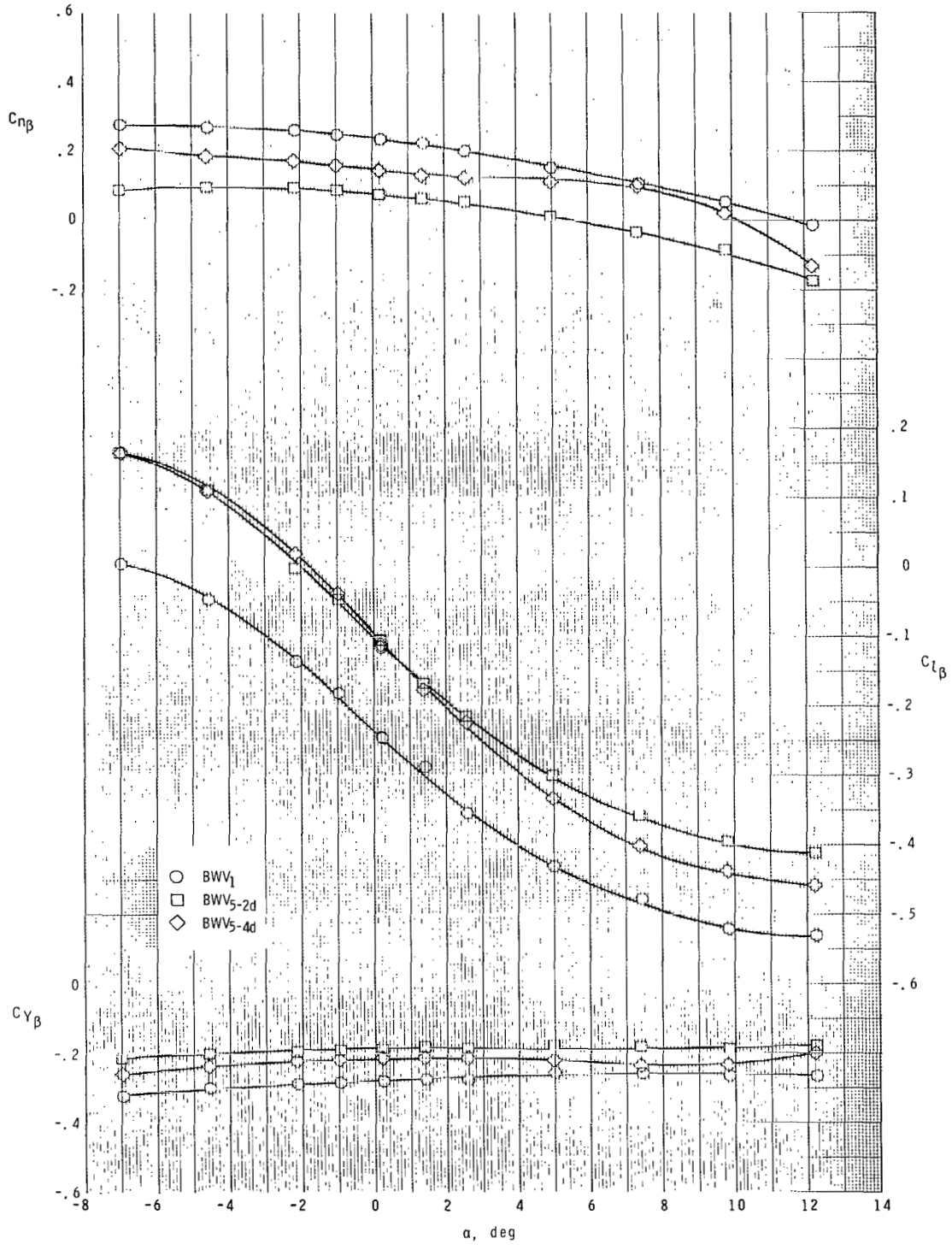

(a) M = 1.60.

Figure 4.- Comparison of half-size wing-mounted vertical tails and single body-mounted vertical tail.

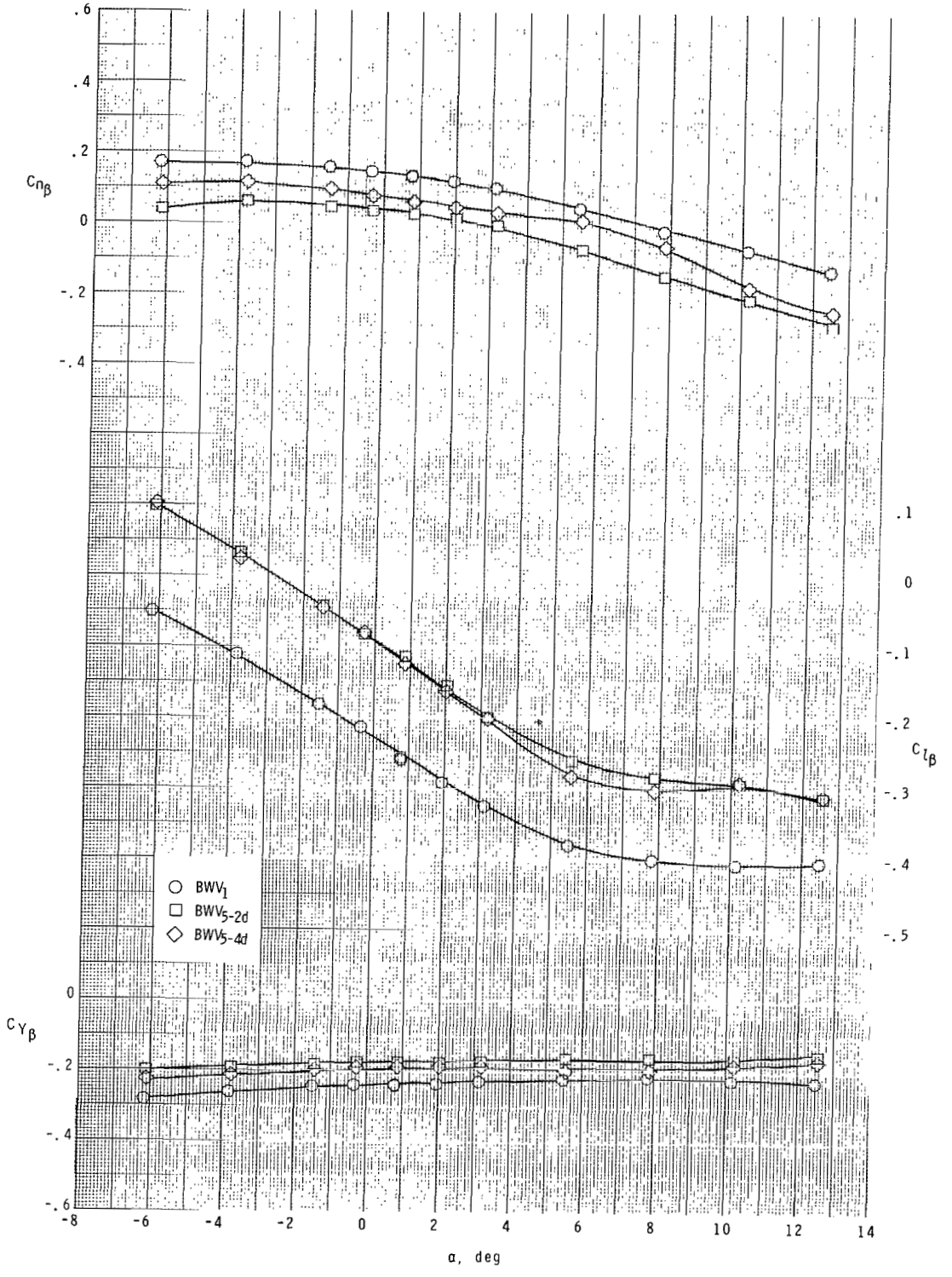

(b) M = 2.00.

Figure 4.- Continued.

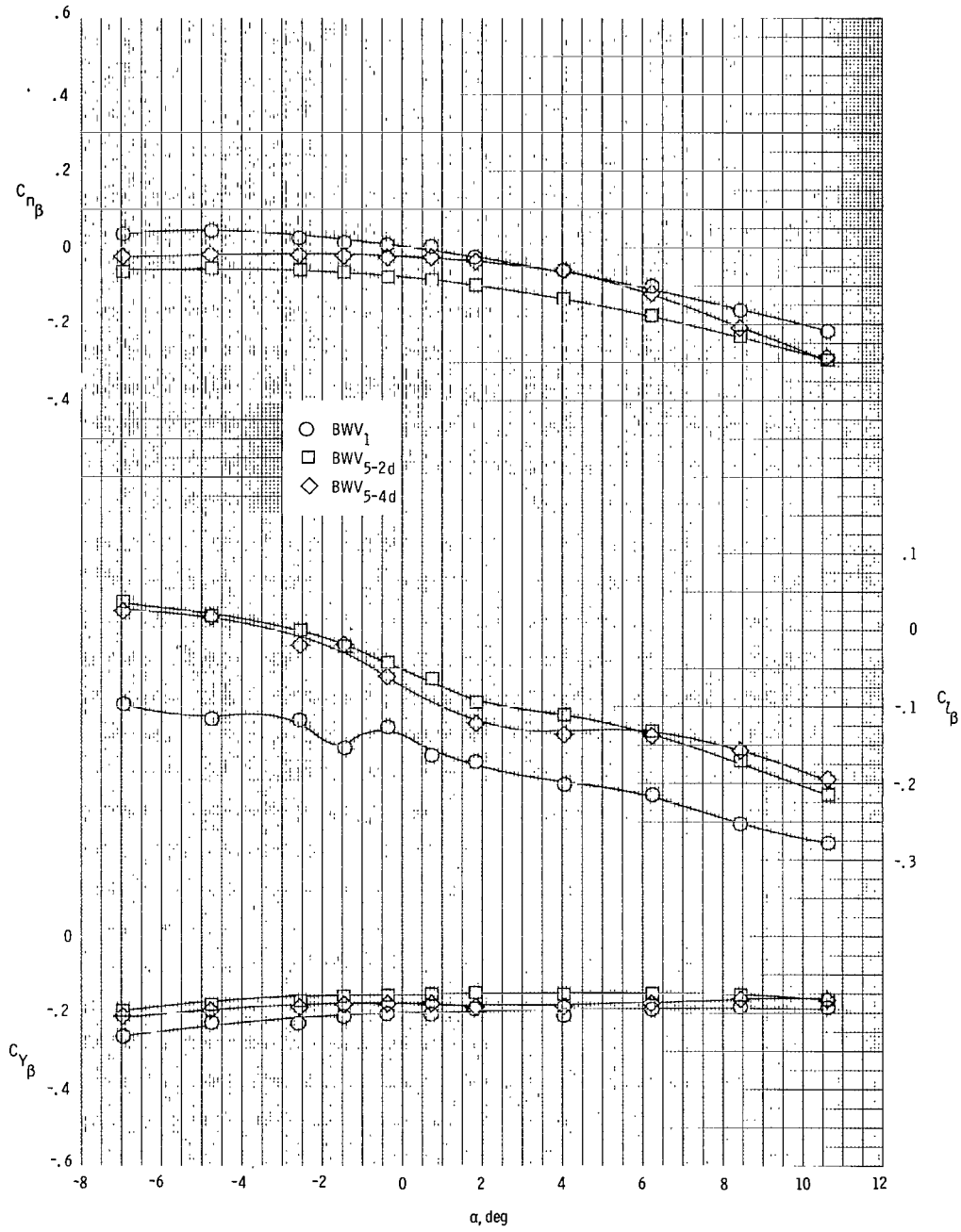

(c) M = 2.86.

Figure 4.- Concluded.

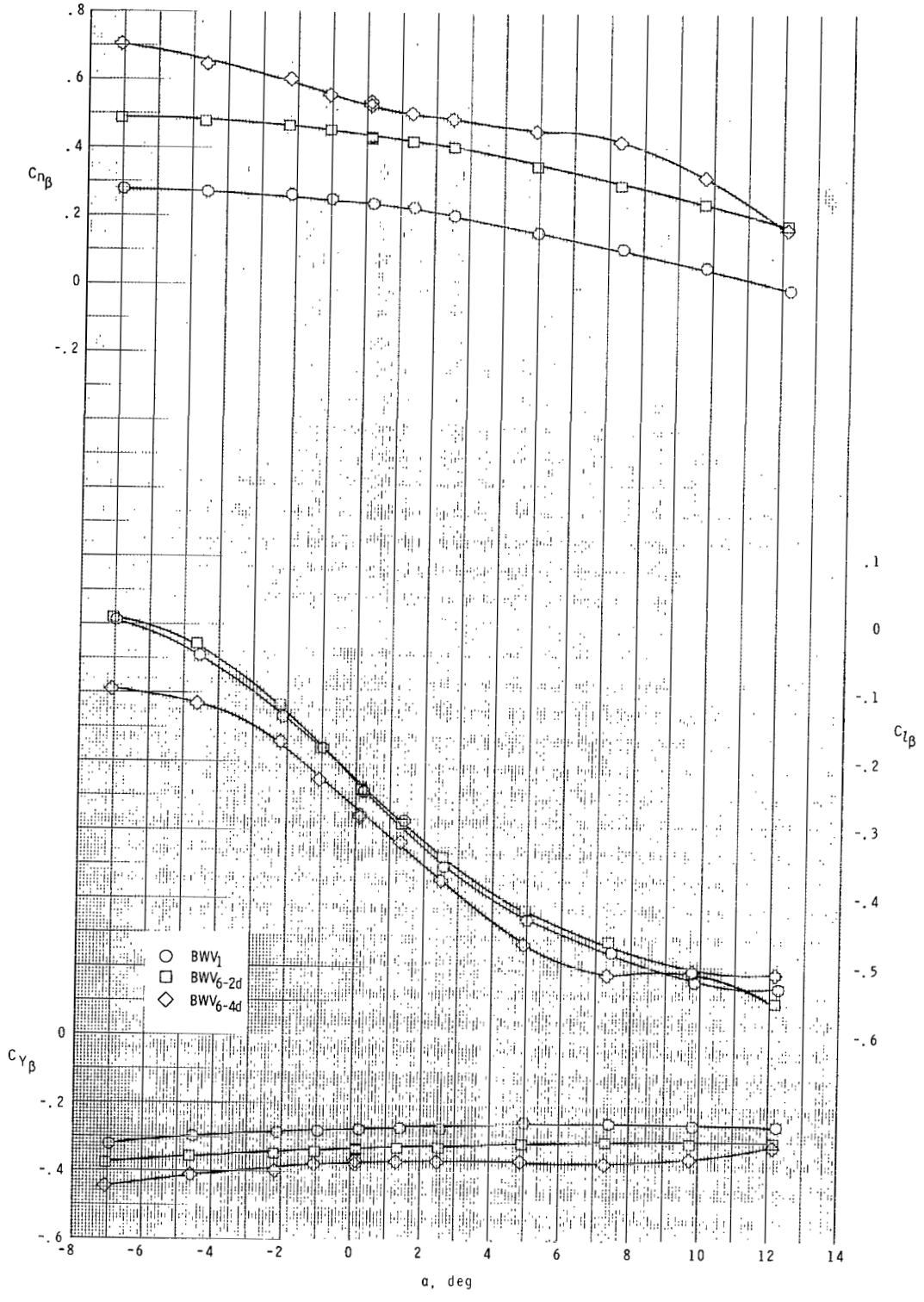

(a) M = 1.60.

Figure 5.- Comparison of full-size wing-mounted vertical tails and single body-mounted vertical tail.

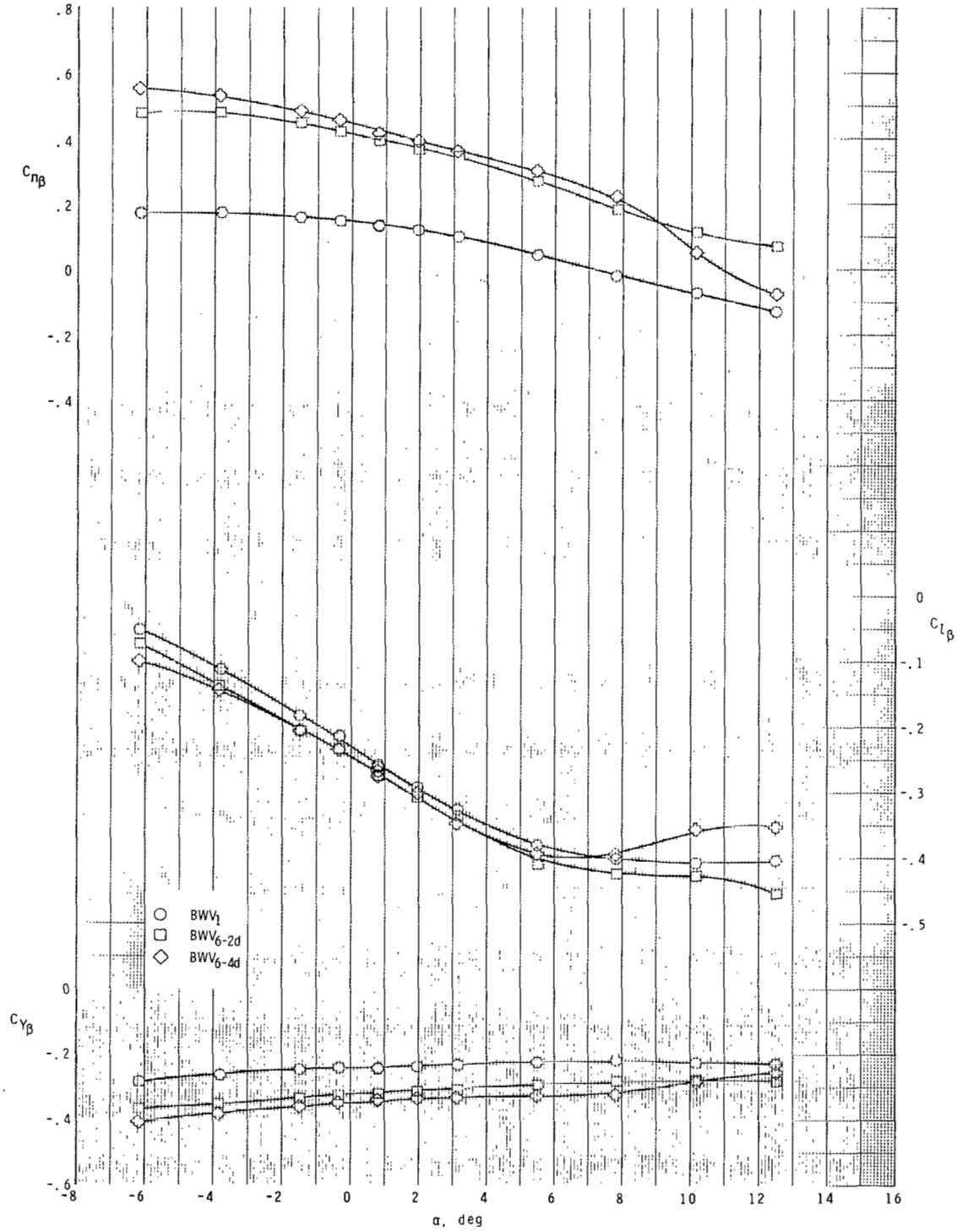

(b) M = 2.00.

Figure 5.- Continued.

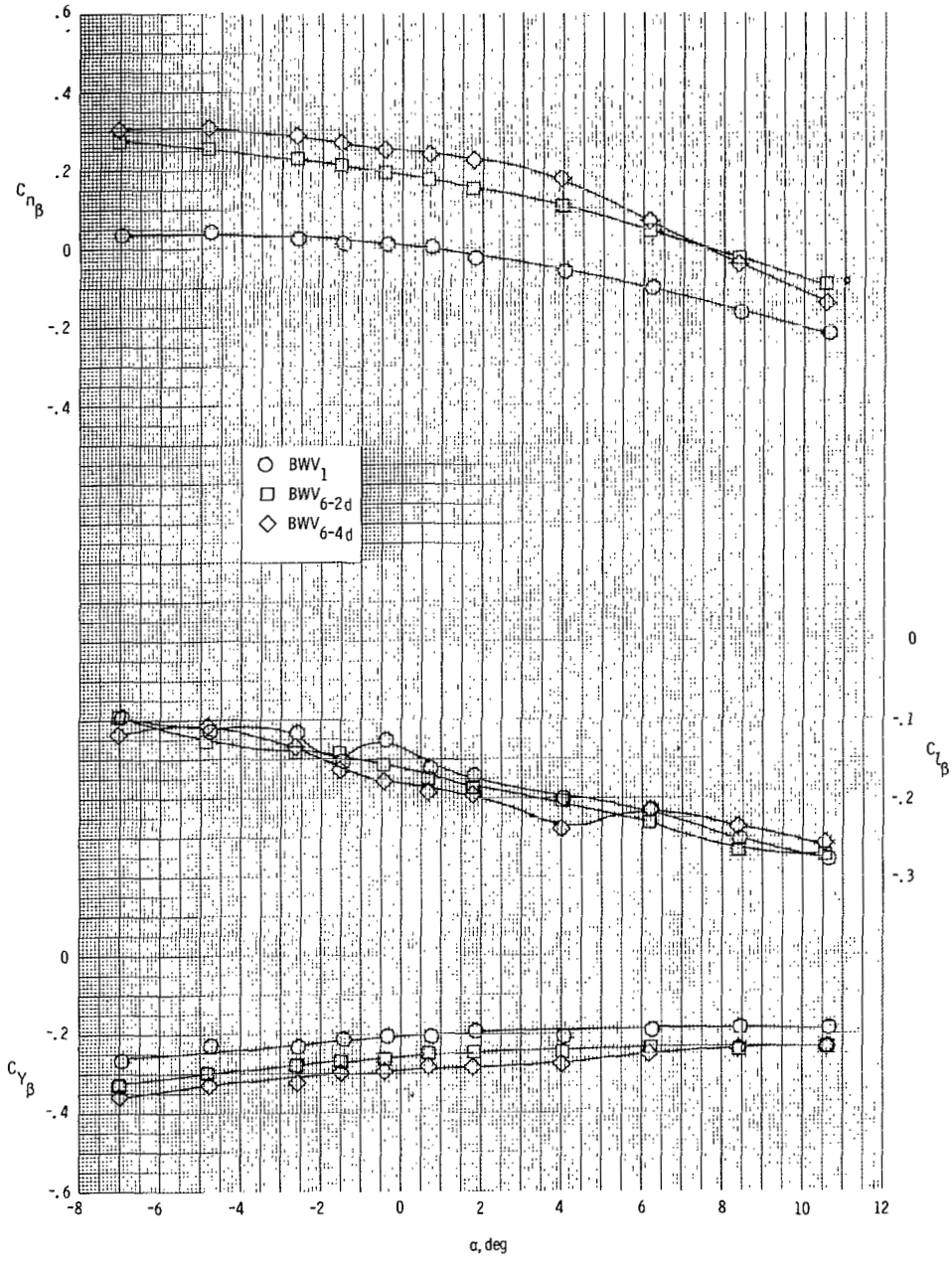

(c) M = 2.86.

Figure 5.- Concluded.

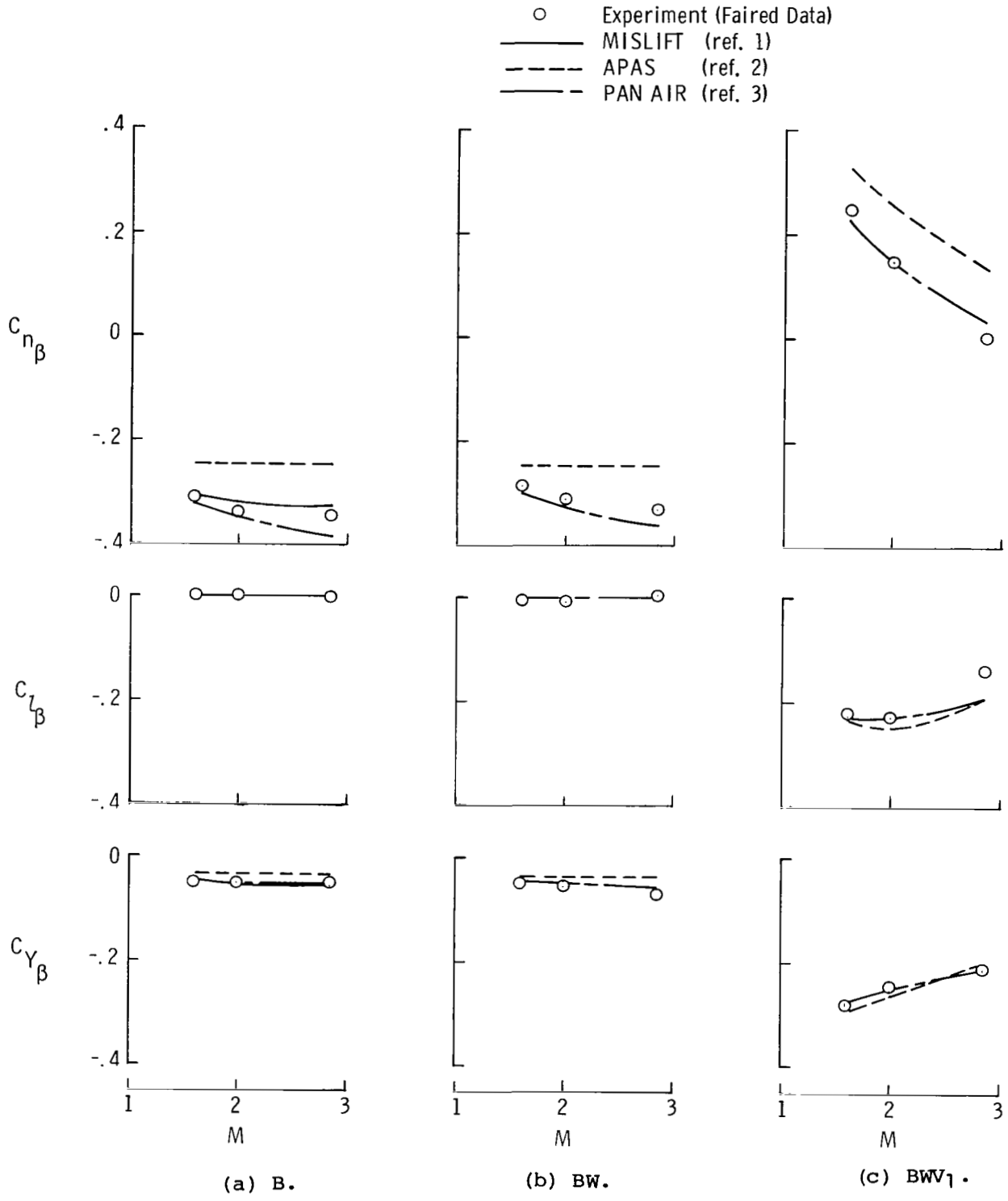

Figure 6.- Comparison of experimental and theoretical lateral-directional stability characteristics at $\alpha = 0^o$.

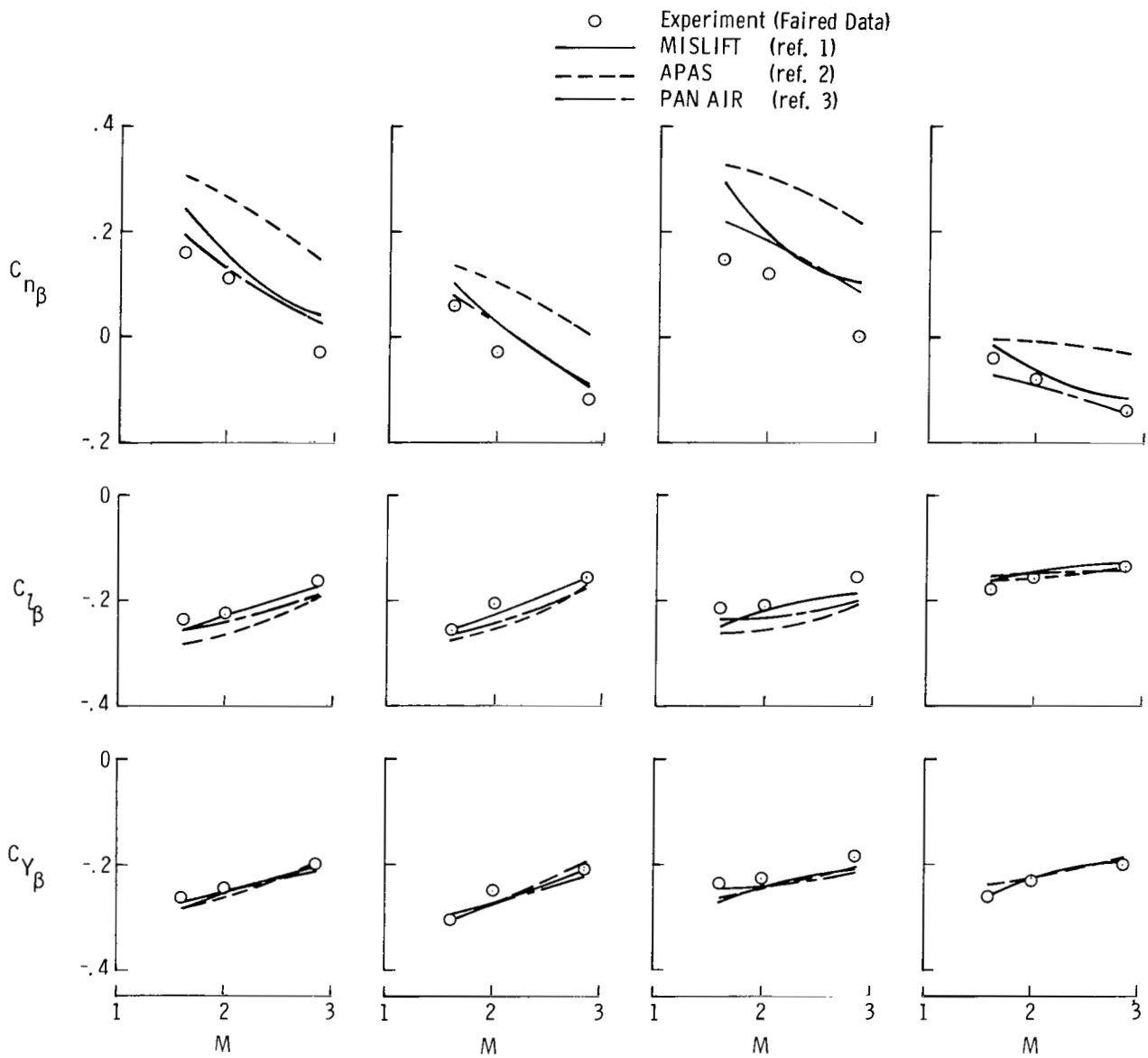

(d) BV_1. (e) BV_2. (f) BV_3. (g) BV_4.

Figure 6.- Continued.

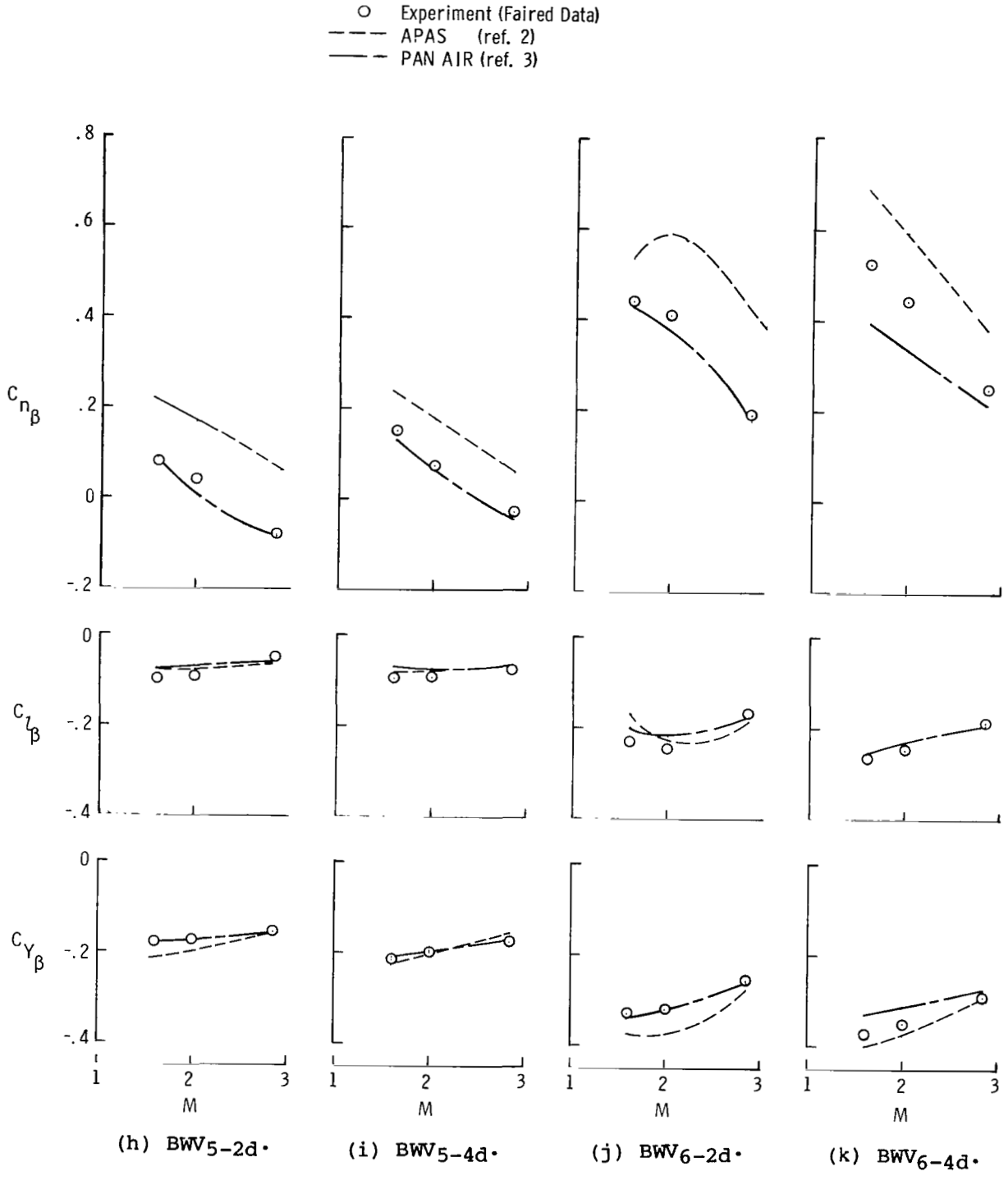

(h) BWV_{5-2d}. (i) BWV_{5-4d}. (j) BWV_{6-2d}. (k) BWV_{6-4d}.

Figure 6.- Concluded.

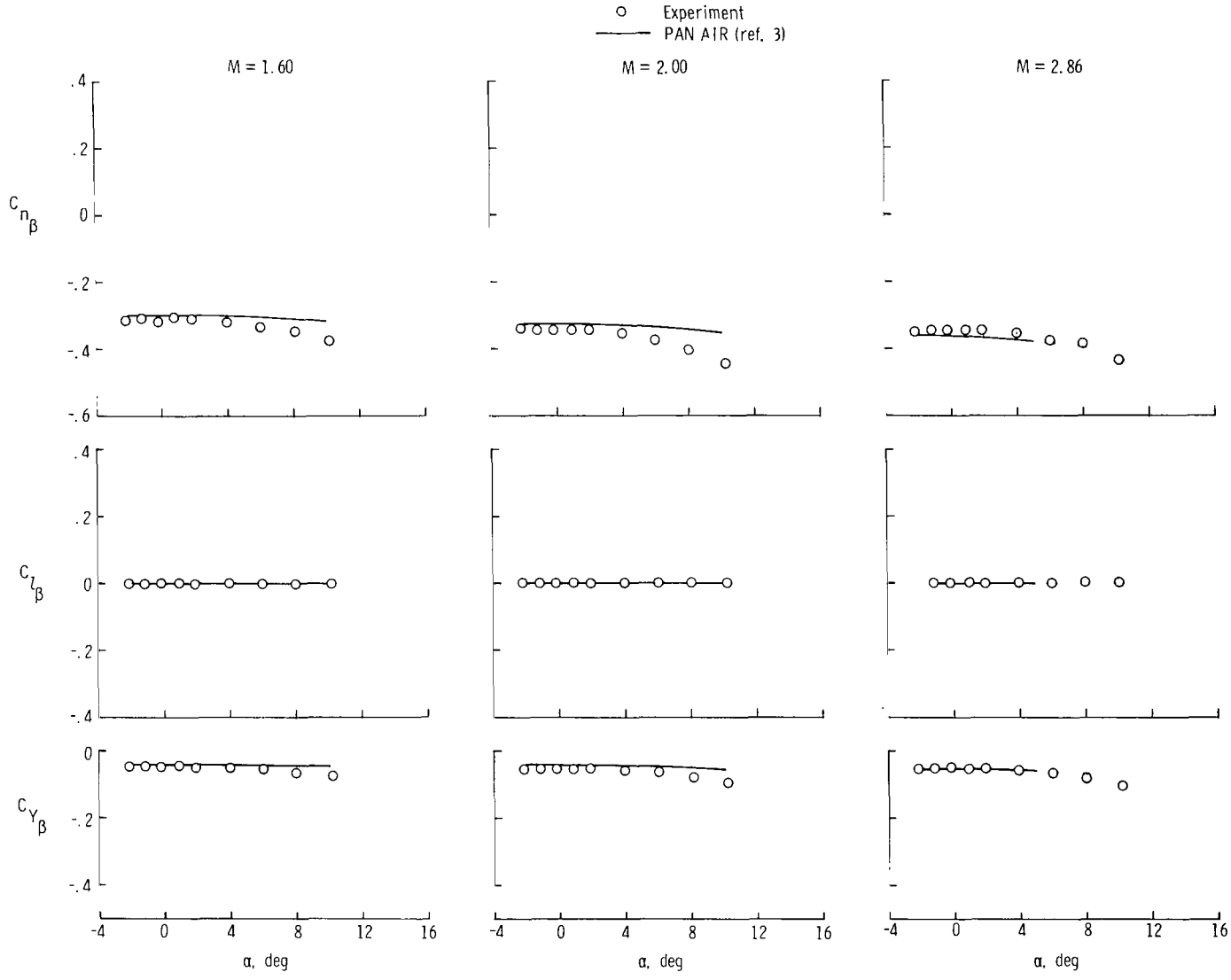

(a) B configuration.

Figure 7.- Comparison of experimental and theoretical lateral-directional stability characteristics at angle of attack.

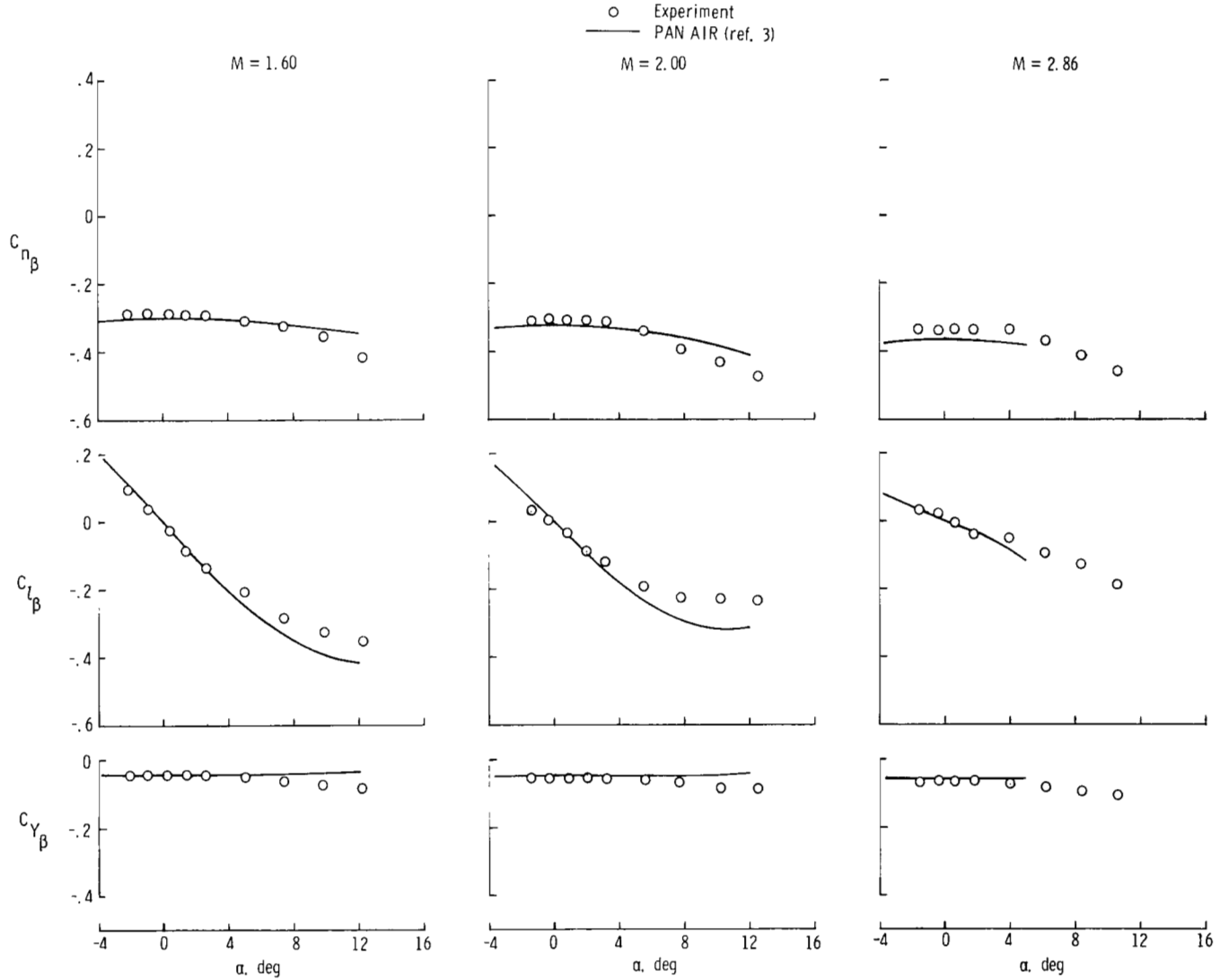

(b) BW configuration.

Figure 7.- Continued.

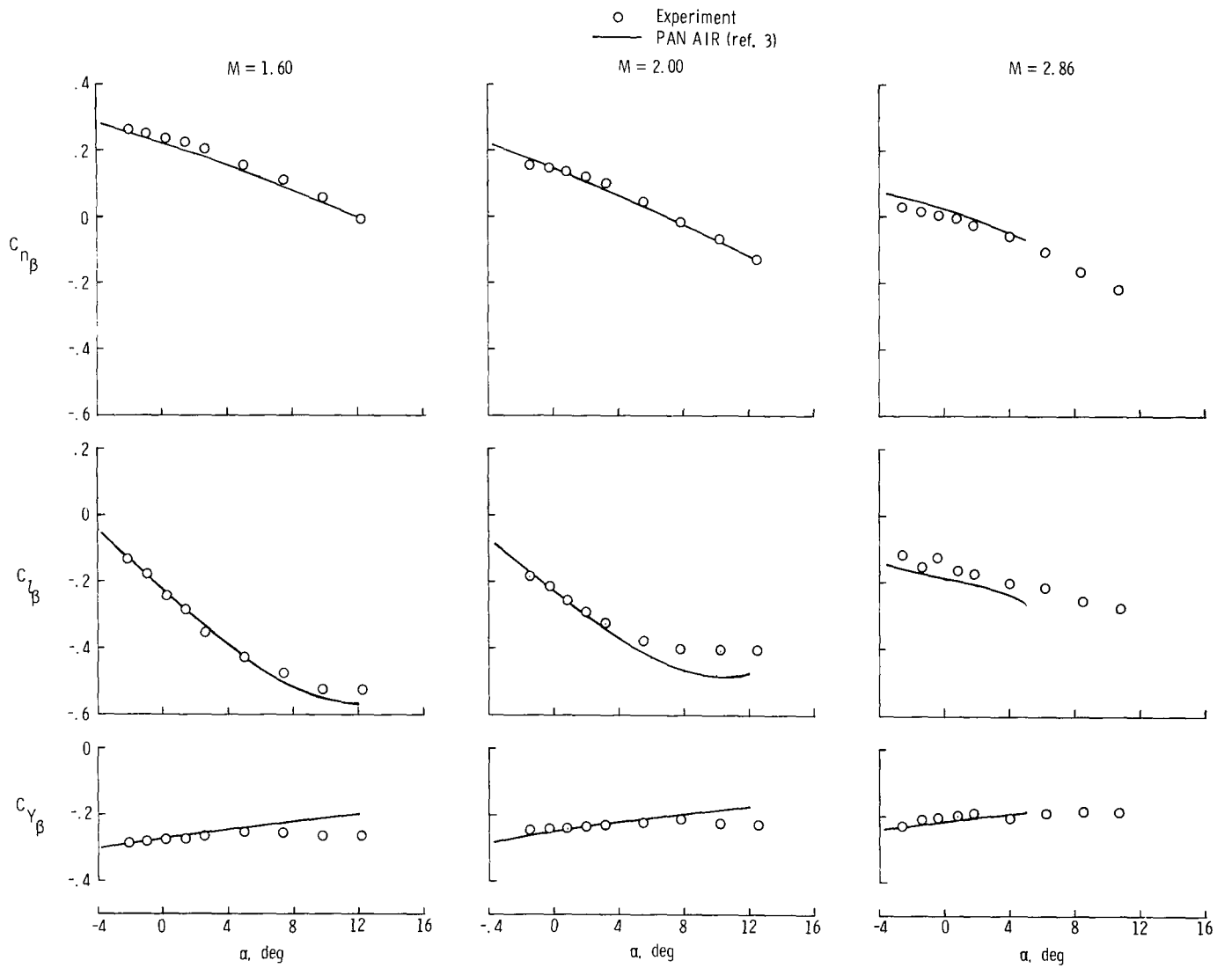

(c) BWV$_1$ configuration.

Figure 7.- Continued.

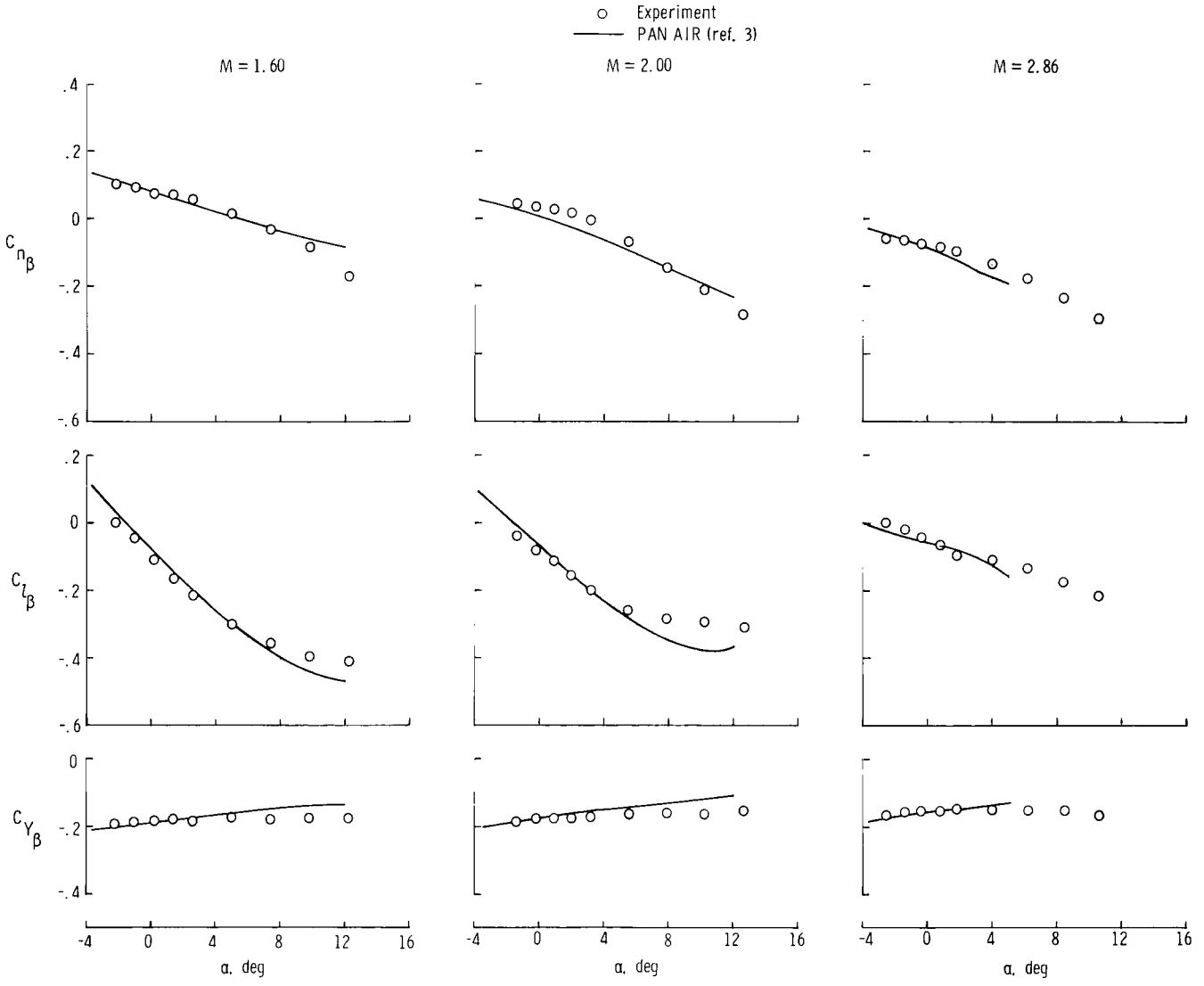

(d) BWV_{5-2d} configuration.

Figure 7.- Continued.

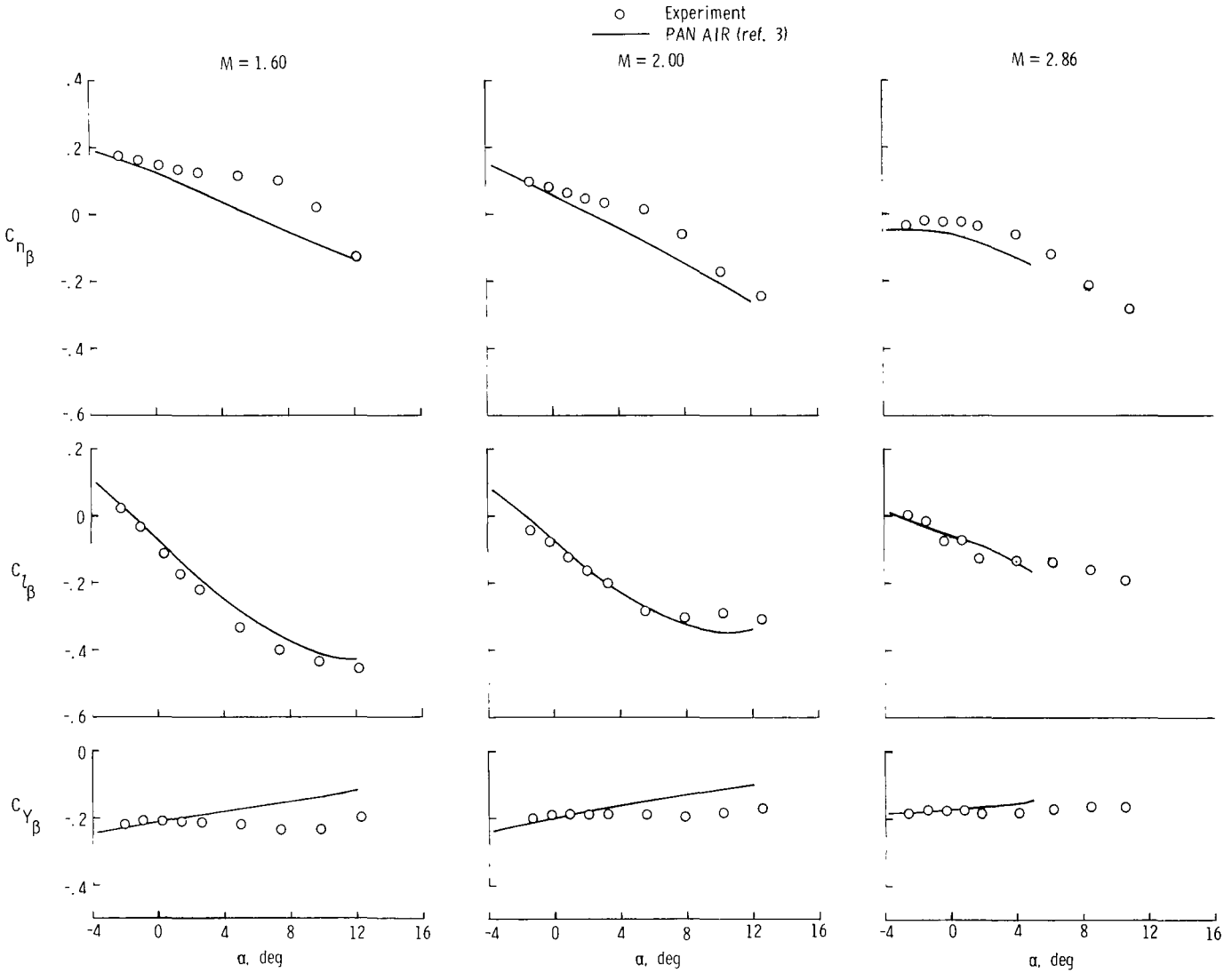

(e) BWV_{5-4d} configuration.

Figure 7.- Continued.

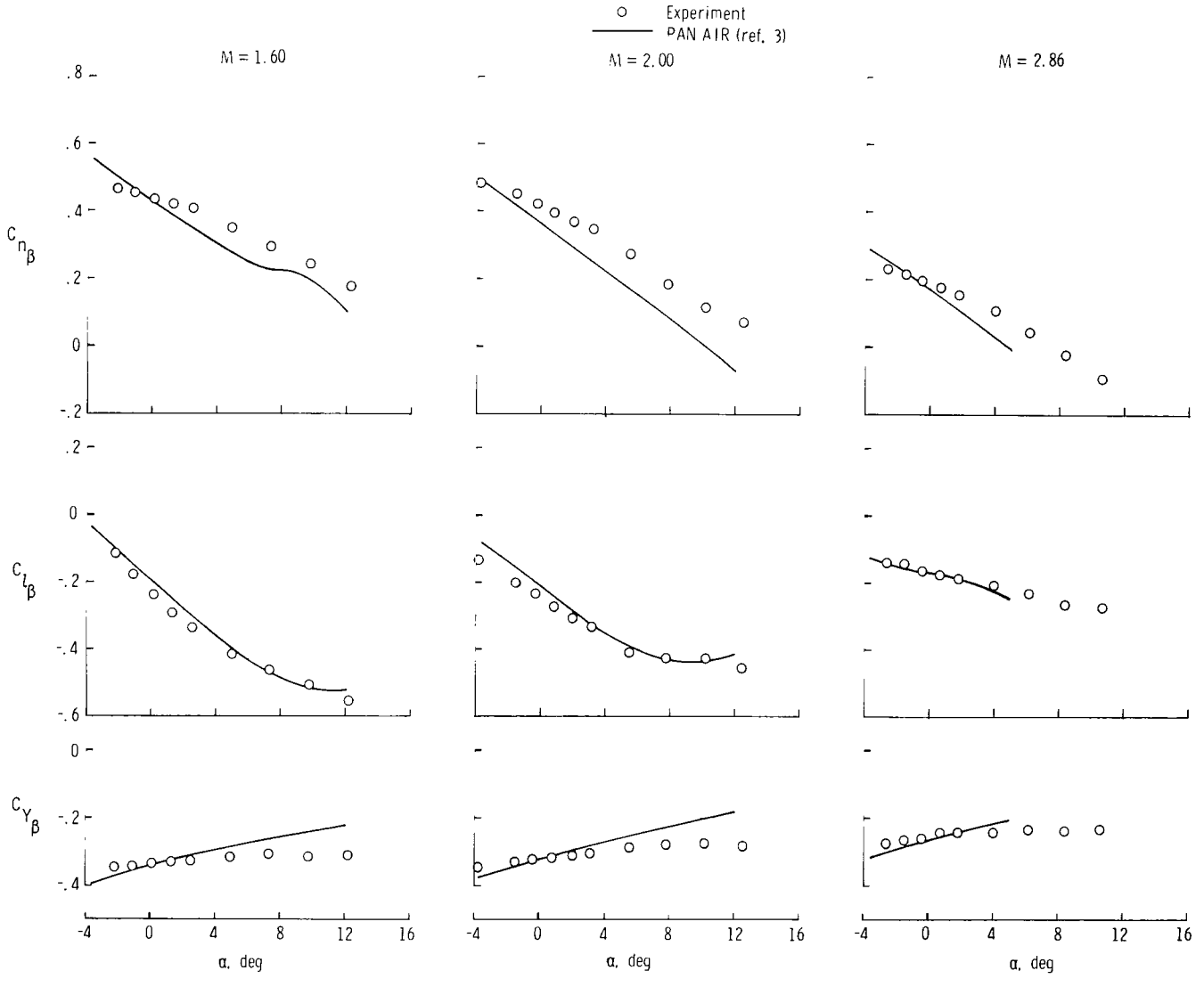

(f) BWV_{6-2d} configuration.

Figure 7.- Continued.

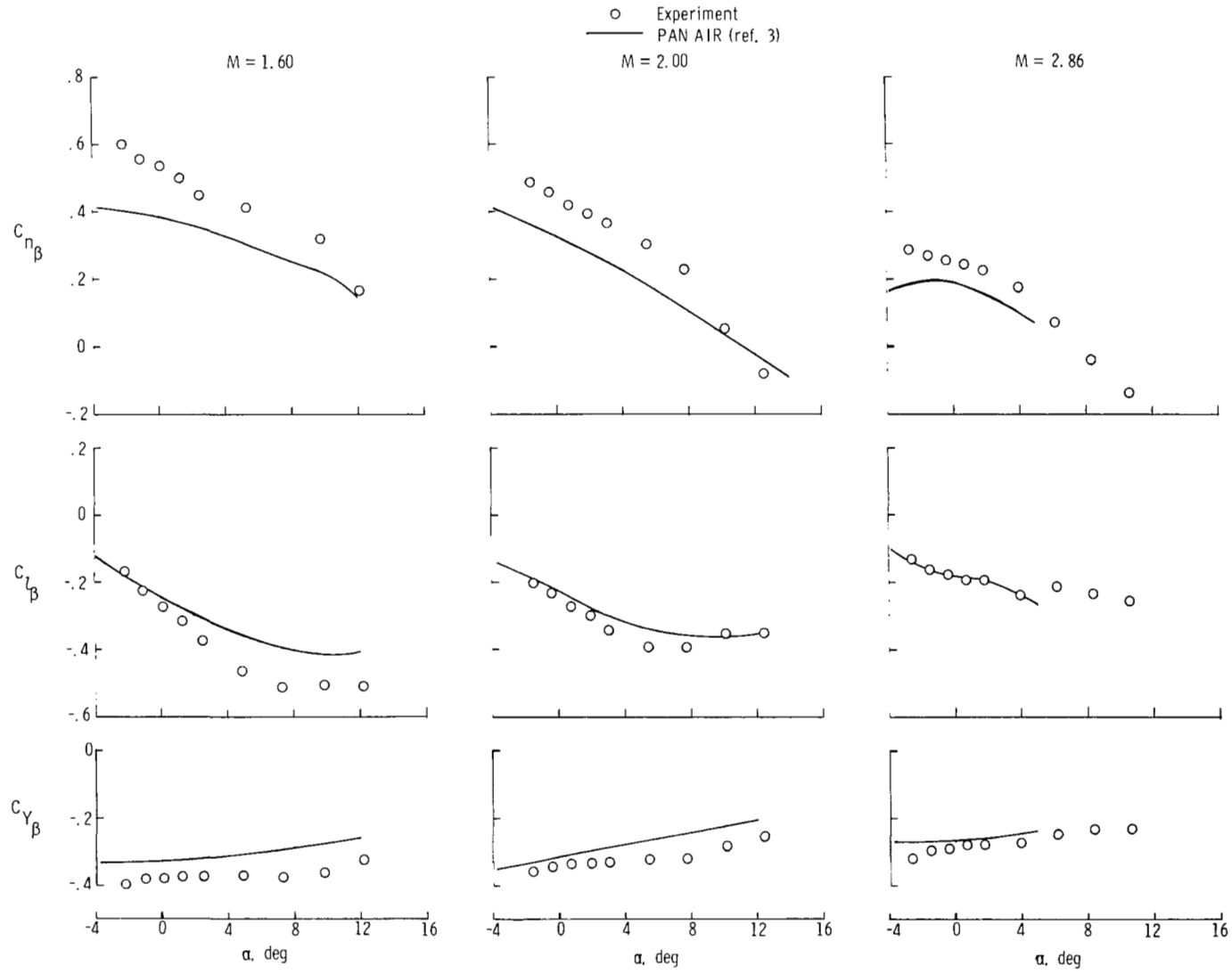

(g) BWV_{6-4d} configuration.

Figure 7.- Continued.

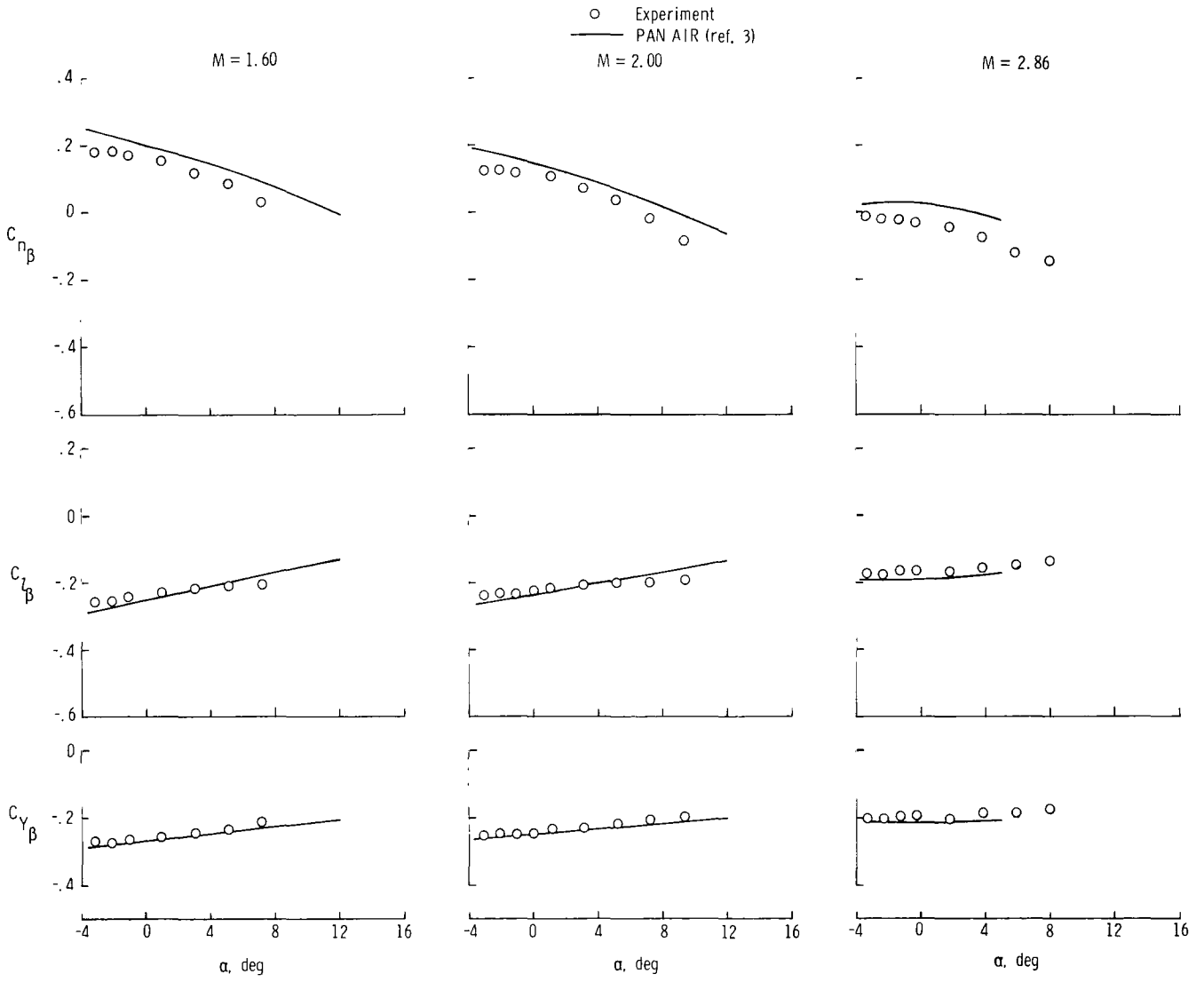

(h) BV_1 configuration.

Figure 7.- Continued.

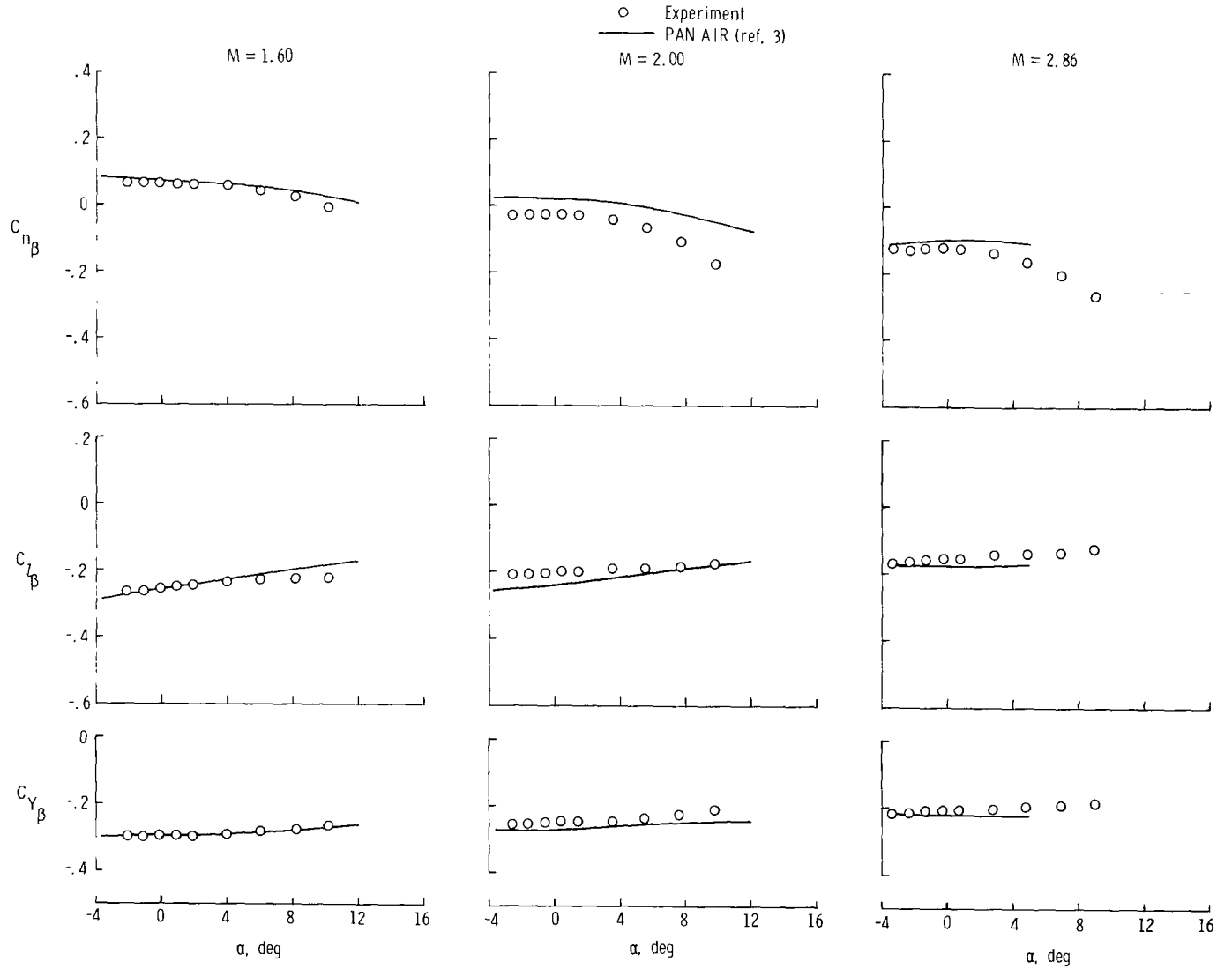

(i) BV_2 configuration.

Figure 7.- Continued.

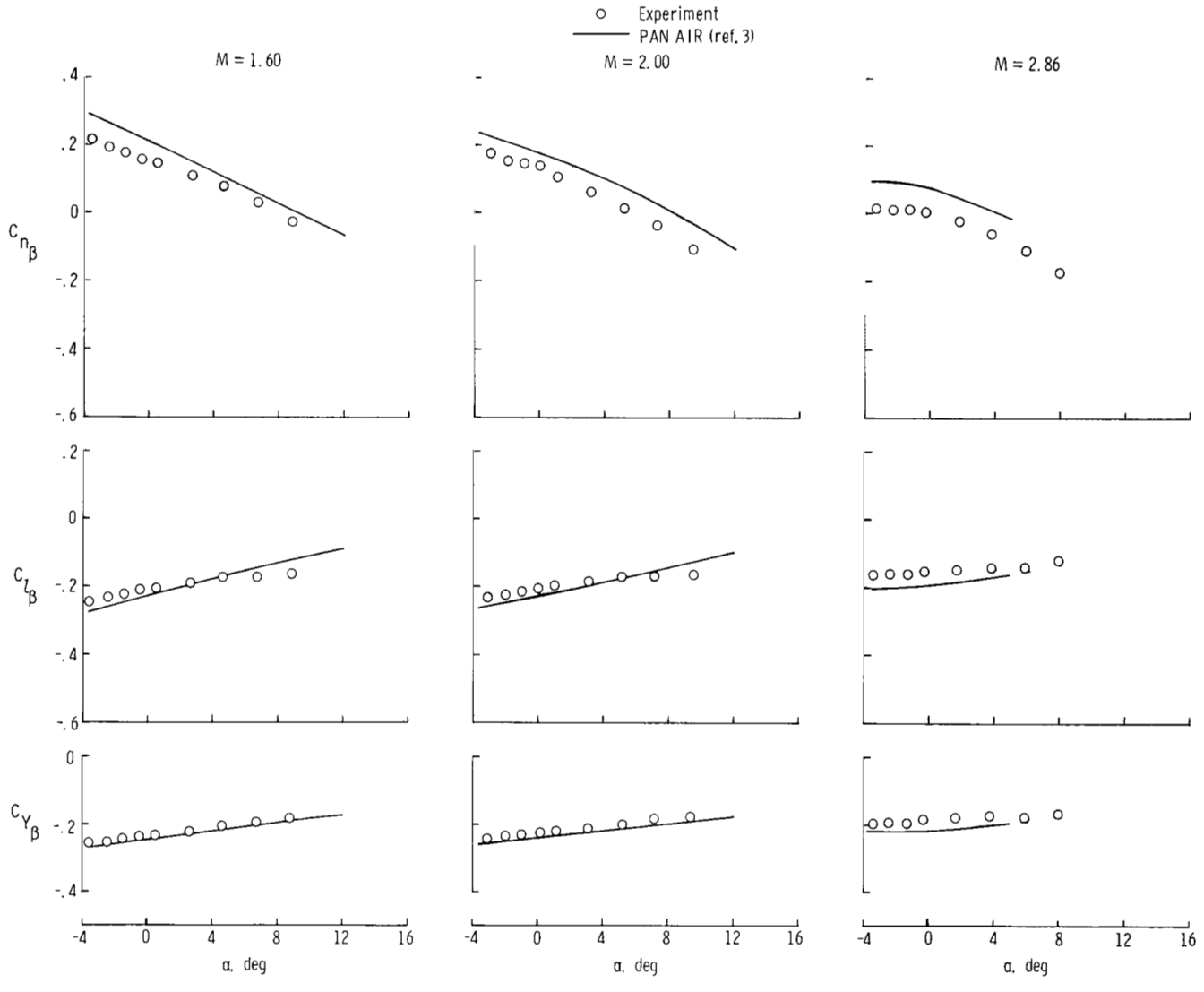

(j) BV_3 configuration.

Figure 7.- Continued.

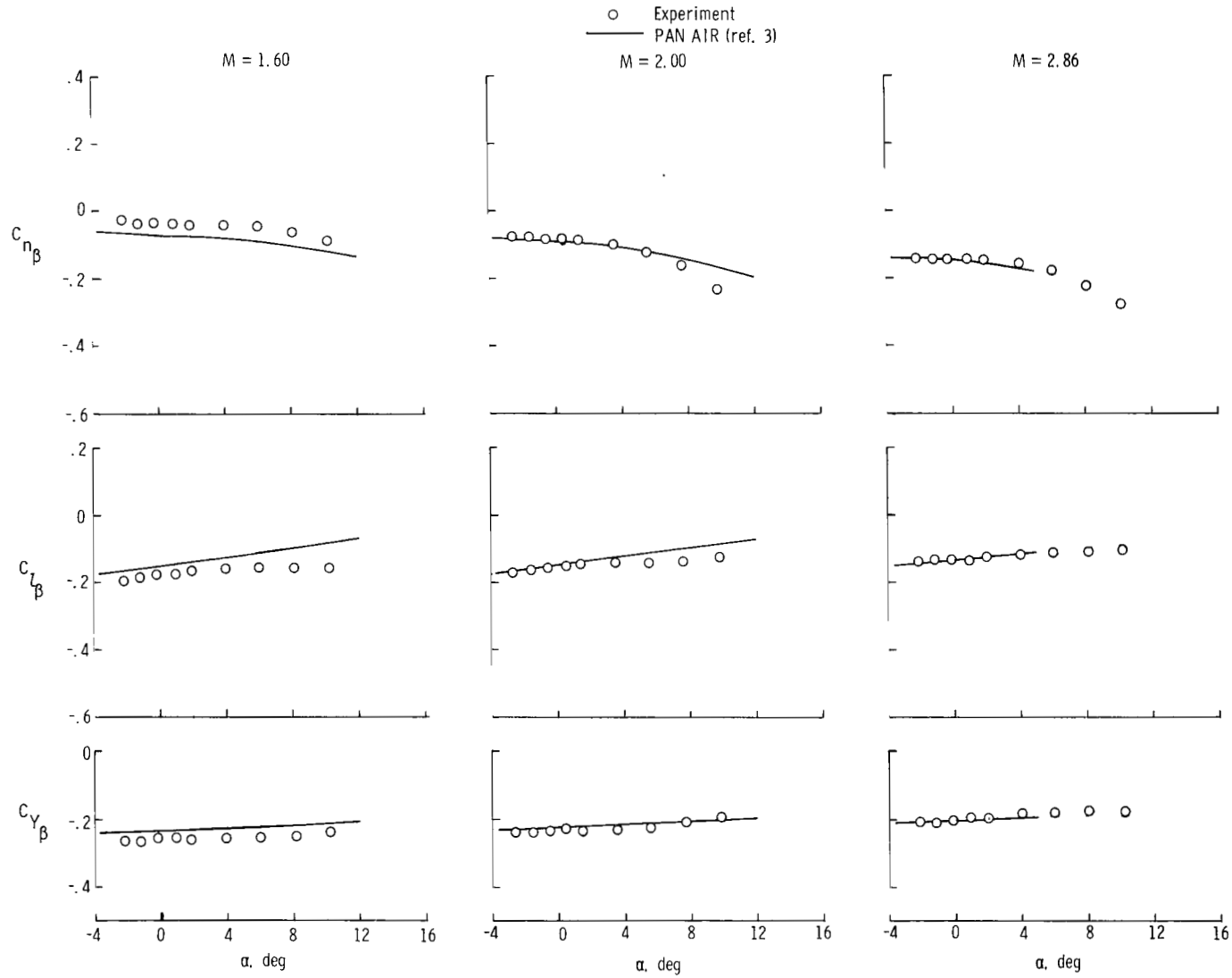

(k) BV_4 configuration.

Figure 7.- Concluded.

1. Report No.	2. Government Accession No.	3. Recipient's Catalog No.
NASA TP-1878		

4. Title and Subtitle	5. Report Date
EXPERIMENTAL AND THEORETICAL SUPERSONIC LATERAL-DIRECTIONAL STABILITY CHARACTERISTICS OF A SIMPLIFIED WING-BODY CONFIGURATION WITH A SERIES OF VERTICAL-TAIL ARRANGEMENTS	August 1981
	6. Performing Organization Code 505-43-23-02

7. Author(s)	8. Performing Organization Report No.
Milton Lamb, Wallace C. Sawyer, and James L. Thomas	L-14328
	10. Work Unit No.
9. Performing Organization Name and Address	
NASA Langley Research Center Hampton, VA 23665	11. Contract or Grant No.
	13. Type of Report and Period Covered Technical Paper
12. Sponsoring Agency Name and Address	
National Aeronautics and Space Administration Washington, DC 20546	14. Sponsoring Agency Code

15. Supplementary Notes

16. Abstract

An experimental investigation has been conducted to provide a systematic set of lateral-directional stability data for a simplified wing-body model with a series of vertical-tail arrangements. The study was made at Mach numbers from 1.60 to 2.86 at nominal angles of attack from -8° to 12° and Reynolds number of 8.2×10^{6} per meter. Comparisons at zero angle of attack have been made with three existing theoretical methods (MISLIFT - a second-order shock expansion and panel method; APAS - a slender body and "first order" panel method; and PAN AIR - a "higher order" panel method) and comparisons at angle of attack have been made with PAN AIR. The results show that PAN AIR generally provides accurate estimates of these characteristics at moderate angles of attack for complete configurations with either single or twin vertical tails. APAS provides estimates for complete configurations at zero angle of attack. However, MISLIFT only provides estimates for the simplest body—vertical-tail configurations at zero angle of attack.

17. Key Words (Suggested by Author(s))

Experimental lateral-directional stability characteristics
Theoretical lateral-directional stability characteristics
Simplified wing—body—vertical-tail configurations
Series of vertical-tail arrangements
Supersonic speed

18. Distribution Statement

Unclassified - Unlimited

Subject Category 02

19. Security Classif. (of this report)	20. Security Classif. (of this page)	21. No. of Pages	22. Price
Unclassified	Unclassified	45	A03

For sale by the National Technical Information Service, Springfield, Virginia 22161

NASA-Langley, 1981

National Aeronautics and
Space Administration

Washington, D.C.
20546

Official Business
Penalty for Private Use, $300

THIRD-CLASS BULK RATE

Postage and Fees Paid
National Aeronautics and
Space Administration
NASA-451

2 1 1U,A, 080481 S00903DS
DEPT OF THE AIR FORCE
AF WEAPONS LABORATORY
ATTN: TECHNICAL LIBRARY (SUL)
KIRTLAND AFB NM 87117

NASA

POSTMASTER: If Undeliverable (Section 158 Postal Manual) Do Not Return